



Australia's National
Science Agency

Hydroclimate and catchment processes impacting runoff in the northern Murray–Darling Basin

Jorge L. Peña-Arancibia, Francis H. S. Chiew, Yingying Yu, and Guobin Fu

MD-WERP Project T2.H.2

June 2023



Citation

Peña-Arancibia JL, Chiew FHS, Yu Y, and Fu G (2023) Hydroclimate and catchment processes impacting runoff in the northern Murray–Darling Basin. CSIRO Technical report for the Murray–Darling Basin Authority. CSIRO, Australia.

Copyright

© Murray–Darling Basin Authority 2022. With the exception of the Commonwealth Coat of Arms, the MDBA logo, the MD–WERP logo, the CSIRO logo, and any trademarks, and any exempt content (if identified), this publication is provided under a Creative Commons Attribution 4.0 licence (CC-BY). CSIRO have all necessary rights and permissions to make this publication available publicly under a CC-BY licence for the purposes of supporting MD-WERP objectives or other research purposes.

Important disclaimer

CSIRO advises that the information contained in this publication comprises general statements based on scientific research. The reader is advised and needs to be aware that such information may be incomplete or unable to be used in any specific situation. No reliance or actions must therefore be made on that information without seeking prior expert professional, scientific and technical advice. To the extent permitted by law, CSIRO (including its employees and consultants) excludes all liability to any person for any consequences, including but not limited to all losses, damages, costs, expenses and any other compensation, arising directly or indirectly from using this publication (in part or in whole) and any information or material contained in it.

CSIRO is committed to providing web accessible content wherever possible. If you are having difficulties with accessing this document please contact [csiro.au/contact](https://www.csiro.au/contact).

Contents

Executive summary	iv
1 Introduction	1
1.1 Background	1
2 Climate and runoff	5
2.1 Rainfall	5
2.2 Evaporative demand.....	8
2.3 Runoff	11
3 Vegetation.....	14
3.1 Actual evapotranspiration	14
3.2 Vegetation phenology	16
4 Groundwater.....	18
4.1 Groundwater level.....	18
4.2 Groundwater storage	19
5 Anthropogenic changes	21
5.1 Irrigation	21
5.2 Farm dams	22
6 Summary and recommendations	25
6.1 Summary.....	25
6.2 Recommendations.....	27
Appendix A Evaluation of alternative actual evapotranspiration models.....	29
Appendix B Other ancillary data	31
References	32

Figures

Figure 1. River valley divisions of the Murray-Darling Basin (southern valleys in blue outline, northern in maroon outline)	2
Figure 2. Murray-Darling Basin (MDBA) hydrological year (July to next June) rainfall anomaly for 1900/01–2021/22 (with 11-year running mean in black).....	5
Figure 3. Spatial distribution of Australian Gridded Climate Dataset (AGCD) rainfall and associated trends in the Murray-Darling Basin (MDBA)	6
Figure 4. Annual (July to next June) Australian Gridded Climate Dataset (AGCD) rainfall anomalies for 1970/71–2021/22 anomalies averaged for landforms (each row) across the Murray-Darling Basin (MDBA).....	7
Figure 5. Budyko framework for annual water and energy balances (source: Trancoso et al. (2016)) and dryness index (PET/P) in the Murray-Darling Basin	9
Figure 6. Spatial distribution of Australian Water Outlook (AWO) evaporative demand (or potential evapotranspiration, PET) and associated trends in the Murray-Darling Basin (MDBA)	9
Figure 7. Annual (July to next June) Australian Water Outlook (AWO) evaporative demand (PET) anomalies for 1970/71–2021/22 averaged for landforms (each row) across the Murray-Darling Basin (MDBA)	10
Figure 8. Spatial distribution of Australian Water Outlook (AWO) runoff and associated trends in the Murray-Darling Basin (MDBA)	12
Figure 9. Annual (July to next June) Australian Water Outlook (AWO) runoff anomalies for 1970/71–2021/22 averaged for landforms (each row) across the Murray-Darling Basin (MDBA)	13
Figure 10. Spatial distribution of ERA5-Land actual evapotranspiration (ET _a) and associated trends in the Murray-Darling Basin (MDBA)	14
Figure 11. Annual (July to next June) ERA5-Land actual evapotranspiration (ET _a) anomalies for 1970/71–2021/22 averaged for landforms (each row) across the Murray-Darling Basin (MDBA)	15
Figure 12. Spatial distribution of MODIS Leaf Area Index (LAI) and associated trends in the Murray-Darling Basin (MDBA).....	17
Figure 13. Annual (July to next June) MODIS Leaf Area Index (LAI) anomalies for 2000/01–2021/22 averaged for landforms (each row) across the Murray-Darling Basin (MDBA)	17
Figure 14. Spatial distribution of groundwater level trend (1971–2021) or Depth to Water Table (DTW) magnitude from 524 boreholes located in the northern Murray-Darling Basin (MDBA) and associated landforms (Fu et al., 2022).....	18
Figure 15. Monthly groundwater storage anomalies from the Gravity Recovery and Climate Experiment (GRACE) Mascon solutions for January 2003 to December 2022 averaged for landforms across the Murray-Darling Basin (MDBA).....	19

Figure 16. Comparison of annual Murray–Darling Basin (MDB) estimated bulk water take (brown bars, MDBA, 2022) against CMRSET V2.2 averaged actual evapotranspiration (ET _a) minus rainfall (from AGCD) (ET _a -P, green bars)	21
Figure 17. CMRSET V2.2 averaged actual evapotranspiration (ET _a) minus rainfall (from AGCD) (ET _a -P, green bars) and mean annual rainfall (blue line) for selected irrigable areas across the northern Murray–Darling Basin (see Figure 1).	22
Figure 18. Annual timeseries (1986–2020) of aggregated farm dam volume density (in GLkm ⁻²) for landforms in the Murray–Darling Basin	23
Figure 19. Annual timeseries (1992–2020) of aggregated farm dam growth rate (in percentage) for landforms in the Murray–Darling Basin	24
Figure A.1 Comparison of actual evapotranspiration (ET _a) products in the MDB.....	29
Figure A.2 Comparison of actual evapotranspiration (ET _a) models against flux tower ET _a data (left panel, CMRSET V2.2, middle ERA5-Land, right PML V2).....	29
Figure A.3 Comparison of actual evapotranspiration (ET _a) timeseries averaged for landforms across the Murray–Darling Basin (MDBA)	30
Figure B.1. Woody vegetation density c.a. 2019. Data from DEA Landcover.....	31

Tables

Table 1. Summary of main datasets, period of analysis, description, and references.....	3
Table 2. Summary of rainfall characteristics in the Murray–Darling Basin (MDB) and associated landforms	8
Table 3. Summary of potential evapotranspiration (PET) characteristics in the Murray–Darling Basin (MDB) and associated landforms	11
Table 4. Summary of runoff characteristics in the Murray–Darling Basin (MDB) and associated landforms	13
Table 5. Summary of actual evapotranspiration (ET _a) characteristics in the Murray–Darling Basin (MDB) and associated landforms.....	16

Executive summary

The objective of this report is to examine the influence of climate and catchment processes on runoff within the Murray-Darling Basin (MDB), with particular attention on the northern Basin and on factors that can alter hydroclimate characteristics and dominant hydrological processes, commonly referred to as 'hydrologic non-stationarity'. This analysis, which concentrates on trends and variability at the annual level, covers the period from 1970/71 to 2021/22. The findings of this study provide an updated assessment of the MDB's hydrological dynamics, complementing previous analyses conducted by the MDBA, CSIRO and Basin State agencies. The key findings from the data synthesis and analysis from the first year of this study are summarised below. This will be followed by more detailed assessments including modelling in the next year.

- Rainfall has declined over most of the MDB, particularly in the northern and southern Basin uplands, where most of the basin's runoff is generated. The decrease is statistically significant during the cool months (May to Oct) and particularly in the southern Basin, impacting runoff generation processes.
- Evaporative demand has statistically significantly increased across the MDB, largely because of the increase in temperature. This increase can amplify the decrease in rainfall and lead to decreased runoff.
- Runoff has mostly decreased across the MDB, with statistically significant declines in the southern Basin uplands and slopes, and the northern Basin uplands. The decline is primarily observed during the cool season.
- Actual evapotranspiration (ET_a) has declined over most of the MDB, except for densely forested areas in the southern MDB uplands. These declines occur throughout the year, indicating a shift towards ecosystem water limitation in some areas.
- The southern Basin exhibits significant "greening" trends (increase in Leaf Area Index (LAI)), while the northern MDB does not show significant changes in vegetation LAI.
- Groundwater level has generally declined in bore observations in some northern MDB valleys, primarily attributed to reduced groundwater recharge from reduced rainfall and groundwater extraction for irrigation, potentially leading to disconnection of the vadose zone from streams.
- GRACE Groundwater Storage (GWS) anomalies indicate a prolonged dry period during the Millennium Drought, followed by wetter conditions during the La Niña years. However, the northern MDB has experienced a consistent drying trend since 2012/13.
- Irrigation water use changed little during the Millennium Drought and the 2017–2019 dry period. The irrigated surface area reduced during the drought but with more water applied to the smaller irrigated area.
- Farm dams across the MDB have shown growth, particularly during the 1990s and the Millennium Drought. However, growth rates have slowed since 2010. Farm dams can contribute to reductions in runoff, especially during low flow periods, and may compound the effects of reduced rainfall and water scarcity in the MDB.

1 Introduction

1.1 Background

In the last 30 years the Murray–Darling Basin (MDB) has experienced some of the lowest rainfall periods since instrumental records began, including the 1997–2009 “Millennium Drought”. In the northern MDB (all catchments that flow into the Darling River north of its junction with the Murray River, Figure 1) the extremely dry period from January 2017 to December 2019 was the lowest on record “...by a substantial margin, breaking records originally set during the Federation Drought in 1900–1902” (BoM, 2020). These exceptionally dry conditions resulted in very low inflows into major reservoirs, and by January 2020 a record low 254 GL out of 4,708 GL (5.4%) was stored in northern Murray–Darling Basin reservoirs (BoM, 2020).

Chiew et al. (2022), in an MD-WERP tactical project, evaluated the causes of reduced flow in the Barwon–Darling River, the major delivery channel for waters out of the northern Basin into the southern Basin and Murray River. The evaluation identified the dry climate of the past two decades and historical water resource development (water infrastructure and water extraction for irrigation and other productive activities) as the main drivers of the reduced flow. The evaluation also highlighted that climate change and catchment development can modify hydroclimate characteristics and dominant hydrological processes (i.e., ‘hydrologic non-stationarity’), which under dry climates can further reduce annual runoff generated from the same amount of annual rainfall (Chiew et al., 2014). These climate-runoff relationships straying from expected ones have been observed in flows in northern Basin catchments, particularly during the Millennium Drought (Amirthanathan et al., 2023; Rassam et al., 2017).

Compared to studies focused on catchments in the southern Basin or similar climatic and biophysical settings in Australia (Deb et al., 2019; Fowler et al., 2022; Peterson et al., 2021; Saft et al., 2016), there have been very few studies on the drivers of hydrological non-stationarity on catchment runoff and inflow into rivers in the northern Basin. Flows are more variable in the northern Basin than in the south (Grafton et al., 2022; MDBA, 2018) because of the highly variable tropical and extratropical summer (December to February) rainfall as opposed to extratropical winter and spring rainfall fronts in the southern Basin (Gallant et al., 2012). Many northern Basin catchments cease to flow during long dry spells and high flow episodes and floods are also common after dry spells. Analyses and related findings in the southern Basin should be evaluated in the northern Basin as its hydrological setting is markedly different and alterations of hydrological influences continue (e.g., farm dams, land cover change). Findings that streamflow in many drier, flatter, mostly grassland southern Basin catchments does not recover long after returning to wetter conditions is of high relevance to the northern Basin (Peterson et al., 2021).

The aim of this study is to assess the reduction in “natural” catchment runoff or streamflow caused by changes in climatic and landscape characteristics. Understanding the dominant drivers contributing to non-stationary processes will in turn inform the development of more robust catchment hydrological models. This is key for understanding future water availability, as Australia is experiencing increased evaporative demand and changed rainfall patterns as a result of climate

change (CSIRO and BoM, 2022), with a projected median decline in mean annual runoff of 20% in the northern Basin under 2°C global average warming (Whetton and Chiew, 2021).

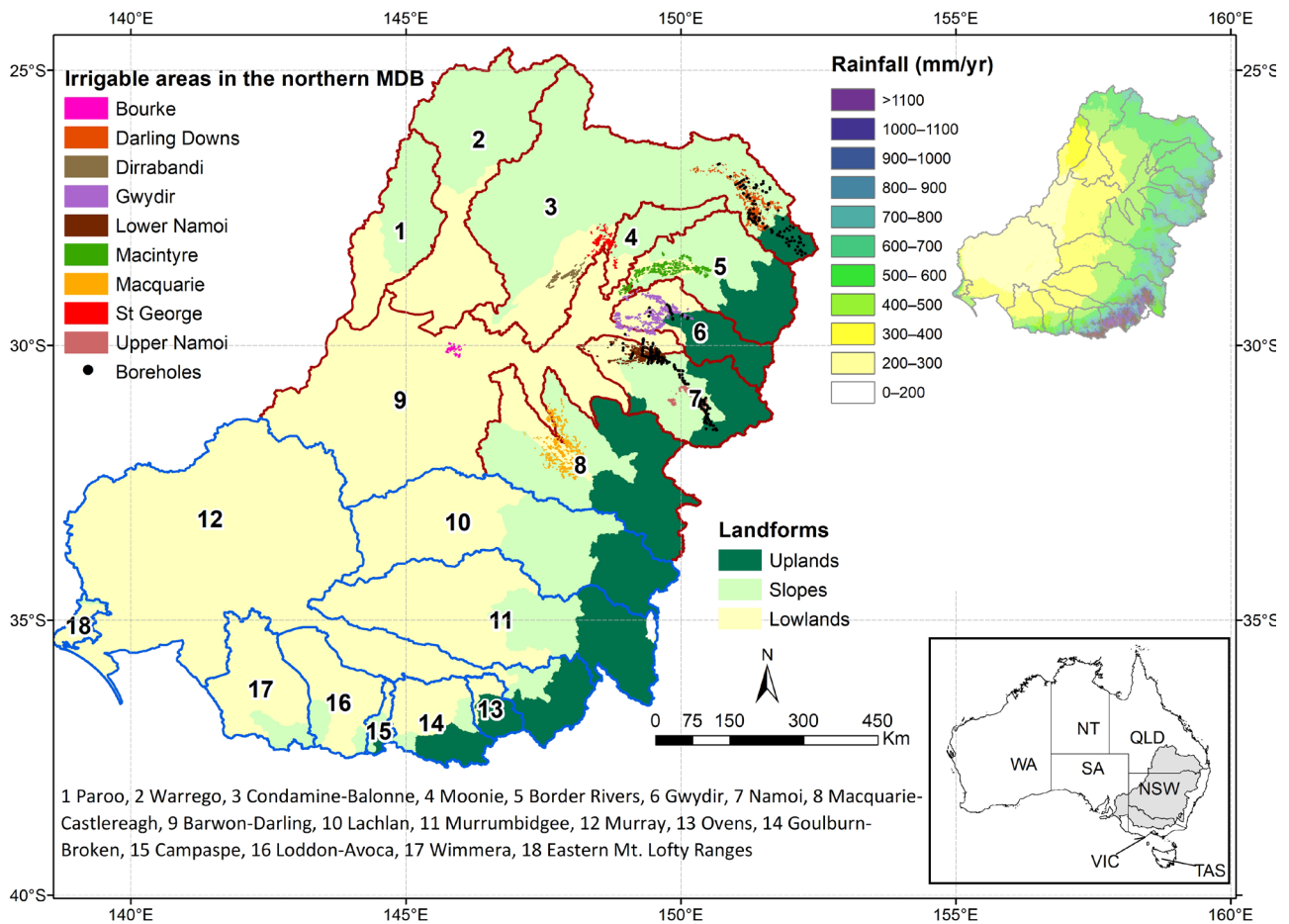


Figure 1. River valley divisions of the Murray-Darling Basin (southern valleys in blue outline, northern in maroon outline), including irrigable areas (coloured by irrigation district), selected groundwater bores and terrain types (landforms) based on topography and elevation. Upper-right inset shows mean annual rainfall for 1970–2018.

This report focuses on recent changes across the MDB that are likely to influence hydrological non-stationarity. This is performed by synthesising, processing, curating and analysing (i) observed hydroclimate data (rainfall, evaporative demand, runoff, groundwater), (ii) remotely sensed data on landscape dynamics (actual evapotranspiration (ET_a), vegetation, groundwater storage) and (iii) data on anthropogenic impacts including irrigation water use and farm dams. This initial analysis, which will be followed by more detailed assessments including modelling in the next year, focuses on observed trends and variability mainly at the annual level (i.e., hydrological year from July to next June, hereafter referred to as annual). The annual timeseries analysis is used to illustrate overall changes in magnitudes and variability, both temporally and spatially. Further analysis will focus on seasonal and event dynamics, which play a key role in processes explanation in the southern Basin (Fowler et al., 2022; Fu et al., 2023). The data used in this study comes mainly from independent operational products providing estimates of key hydrological variables over the long-term (i.e., two or more decades). Table 1 provides a summary of key data sources and analysis periods used in this assessment.

Table 1. Summary of main datasets, period of analysis, description, and references.

VARIABLES	PERIOD	DESCRIPTION	REFERENCE
Rainfall	1970/71–2021/22	Australian Gridded Climate Data (AGDC) rainfall with a spatial resolution of 0.05°.	Evans et al. (2020)
Evaporative demand	1970/71–2021/22	Daily gridded areal potential evapotranspiration for Australia with a spatial resolution of 0.05° calculated using the Morton wet-environment algorithm in the Complimentary Relationship Areal Evaporation (CRAE) model (Morton, 1983). Data from the Australian Water Outlook (AWO).	Frost and Shokri (2021)
Actual evapotranspiration	1970/71–2021/22	Hourly global gridded actual evapotranspiration from ERA5-Land with a spatial resolution ~0.1°	Muñoz-Sabater et al. (2021)
Runoff	1970/71–2021/22	Daily gridded runoff for Australia with a spatial resolution of 0.05° calculated from the Australian Landscape Water Balance model version 7 (AWRA-L v7). Data from the Australian Water Outlook (AWO).	Frost and Shokri (2021)
Groundwater level	1971–2021	Quality-controlled depth to water table (DTW) bore data for Australia from the National Groundwater Information System (NGIS) Version 1.7.0.	BoM (2021)
Groundwater storage anomaly	2003–2022	Monthly global Gravity Recovery and Climate Experiment (GRACE) Mascon with Coastline Resolution Improvement (CRI) filter equivalent water thickness anomalies with a spatial resolution of 0.5°.	Wiese et al. (2016)
Leaf Area Index	2000/01–2021/22	8-day global MOD15A2H V6.1 MODIS combined Leaf Area Index (LAI) with a spatial resolution of ~0.05°.	Knyazikhin et al. (1998)
Farm dam development	1986–2020	Year of commission and spatial location for 727,081 farm dams in the Murray–Darling Basin.	Malerba et al. (2021)
Actual evapotranspiration from irrigable areas	200001–2021/22	Monthly averaged actual evapotranspiration from irrigable areas in the Murray–Darling Basin.	Guerschman et al. (2022)

The analyses are generally performed for the entire MDB. Besides some analyses performed at the pixel scale (of the relevant product), results are also aggregated for the northern and southern MDB which in turn are disaggregated by landforms (see GA, 2008) as follows (see also Figure 1): uplands (generally upland catchments where most of the MDB’s runoff is generated), slopes, and lowlands (where floodplains are located). The analysis period is generally from the 1970/71 to 2021/22, except for some remotely sensed products for which data are only available from the 2000s (see Table 1). The analyses of trends and anomalies (i.e., removing the annual average to highlight periods above/below the mean) are performed from 1970/71 to 2021/22 or the entire period until 2021/22 in the case of remote sensing products. This baseline is adopted to reflect the changing climate (WMO, 2017) and improvements in the density of observational networks (Evans et al., 2020). In addition, the start year and end year of the trend analysis are above average in terms of rainfall, and the start year concurs with changes in the location of droughts and wet hotspots since the 1970s (Verhoeven et al., 2022). Trends are computed using the Mann-Kendall (Kendall, 1975) test and the associated regression coefficients are based on Theil-Sen estimators (Sen, 1968).

It is noted that as the datasets used in the analysis are independent and derived from different observation techniques, retrieval algorithms or obtained through modelling, there is considerable uncertainty in the different variables of the water balance (particularly ET_a). In the semi-arid MDB, runoff is the difference of two large water balance variables, rainfall and ET_a , the errors in these independent datasets result in a lack of water balance closure. Notwithstanding the errors, the emphasis of this analysis is in using diagnostic datasets that include landscape dynamics which can reveal spatiotemporal differences in hydrological catchment functioning. A more comprehensive evaluation of the water balance and its components will be performed next year.

Firstly, Section 2 focuses on changes in climate inputs rainfall, evaporative demand, and runoff. Section 3 follows with changes in vegetation dynamics. This includes ET_a (which is the second largest water balance term after rainfall) and changes in vegetation phenology through Leaf Area Index (LAI). Section 4 describes changes in groundwater level and groundwater storage. Lastly, Section 5 focuses on anthropogenic impacts like irrigation and farm dam development. Section 6 provides a summary and recommendations.

2 Climate and runoff

2.1 Rainfall

Spatiotemporal rainfall variability in the MDB is high compared to other basins worldwide due to the influence of many climate drivers (Gallant et al., 2012; Nicholls et al., 1997). In the MDB the first half of the 20th century experienced mostly drier than average conditions, followed by generally wet years in the 1950s and the 1970s (Figure 2). Annual rainfall in the last two decades in the MDB has been dominated by dry years, except for La Niña years in 2010/11 and 2011/12 and from 2020/21 to 2022/23 (Figure 2).

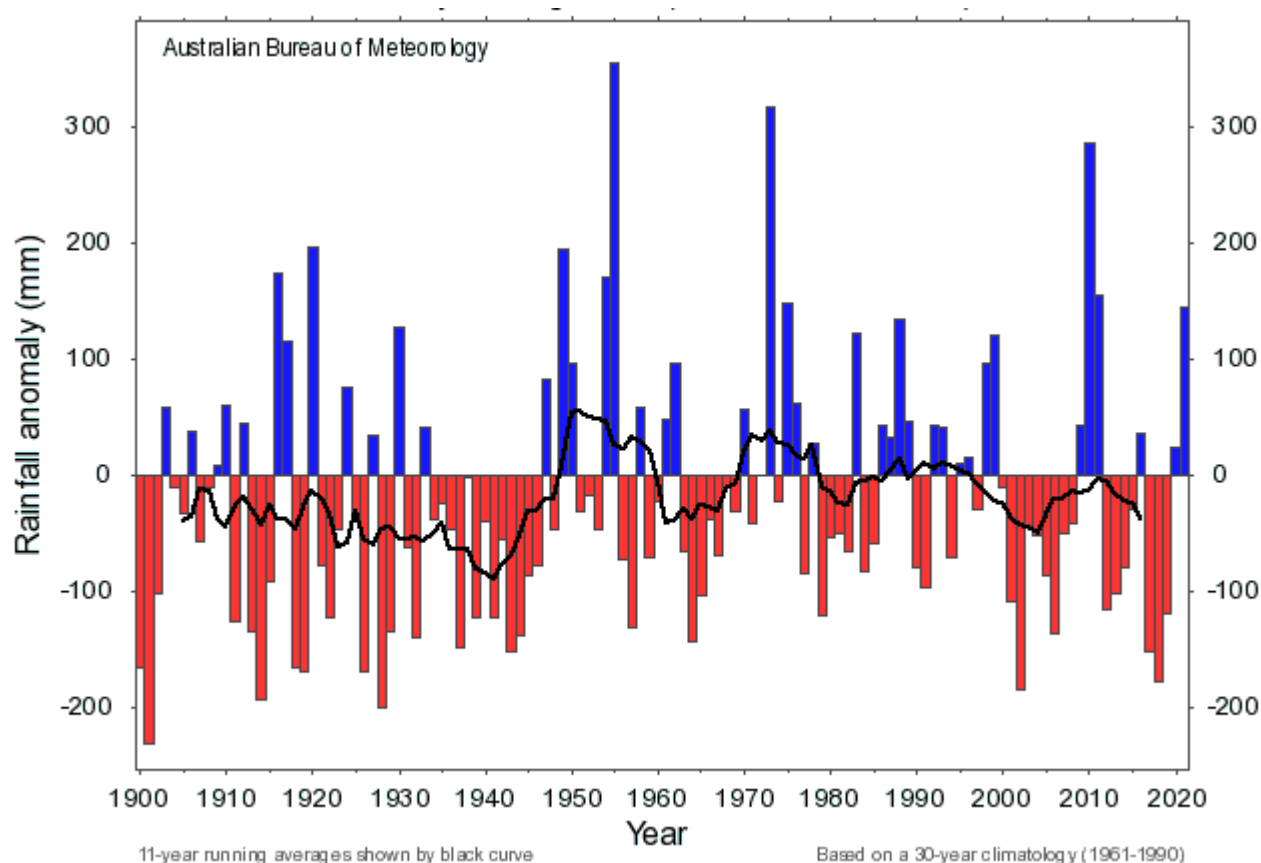


Figure 2. Murray–Darling Basin (MDBA) hydrological year (July to next June) rainfall anomaly for 1900/01–2021/22 (with 11-year running mean in black). Anomaly based on 30-year climatology (1961–90). Source: Bureau of Meteorology website <http://www.bom.gov.au/climate/>.

Basin averaged mean annual rainfall (1970/71–2021/22) is about 480 mm^{-1} , with high spatial (Figure 3) and temporal (Figure 4) variations. Annual rainfall $>2,000 \text{ mm}^{-1}$ occurs in the mountainous areas in the southeast, whereas rainfall is around 300 mm^{-1} in the Basin’s west. The coefficient of variation on annual rainfall (standard deviation divided by the mean, expressed in percentage) is 22%. Mean annual rainfall in the northern MDB is about 500 mm^{-1} (range $241\text{--}1,236 \text{ mm}^{-1}$) and around 455 mm^{-1} (range $210\text{--}2,142 \text{ mm}^{-1}$) in the southern Basin. About 310 mm (62%) falls in the northern basin during the warm months (November to March).

Conversely, about 250 mm (55%) falls in the southern Basin during the cool months (April to October). These months, i.e., November to March in the northern basin, and April to October in the southern Basin, define the wet seasons in these respective parts of the MDB, although some areas experience similar amounts of cool and warm season rainfall.

Trends calculated for 1970/71–2021/22 show mostly declines in annual rainfall (Figure 3), with significant declines ($p < 0.1$) of around $2 \text{ mm}\cdot\text{yr}^{-2}$ estimated in parts the northern Basin uplands, amounting to a decline of about 104 mm in 52 years. Similarly, significant declines ($p < 0.1$) of around $3 \text{ mm}\cdot\text{yr}^{-2}$ are estimated in parts of the southern Basin uplands. This is a decline of about 156 mm over 52 years in these areas. There are also significant declines in the southern Basin slopes in the south.

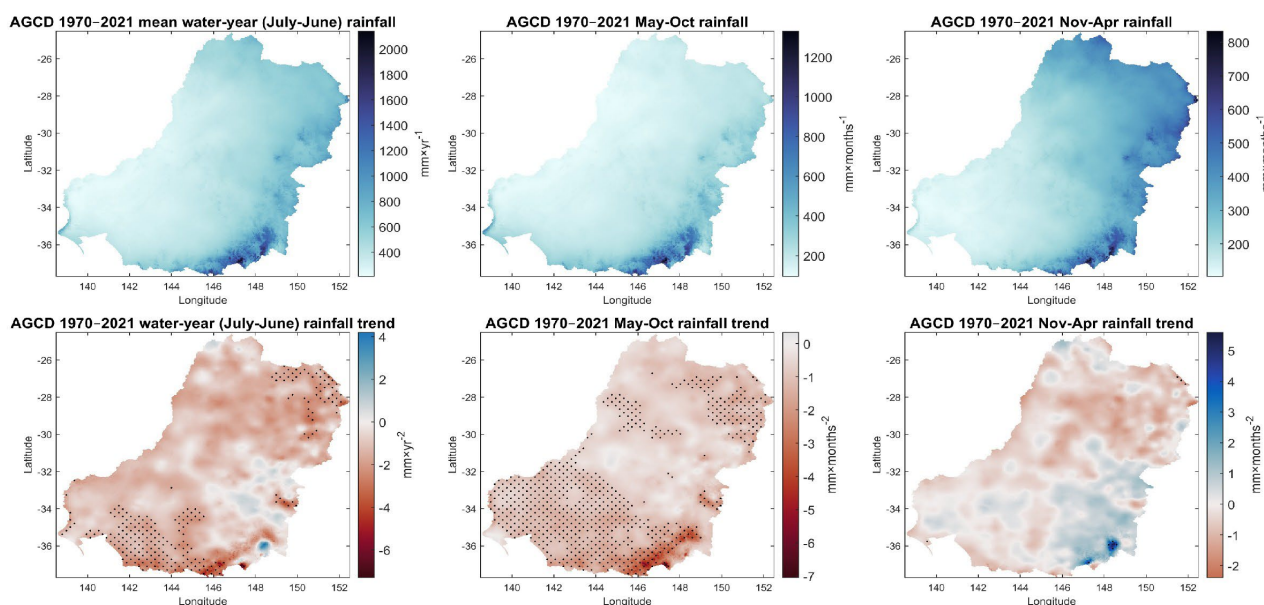


Figure 3. Spatial distribution of Australian Gridded Climate Dataset (AGCD) rainfall and associated trends in the Murray–Darling Basin (MDBA). The first column shows mean annual (July to next June) rainfall, the middle column May to October rainfall (i.e., the cool months), and the third column November to next April rainfall (i.e., the warm months). The stipple (black dots) shows 0.05° pixels with significant trends ($p < 0.1$). Note the different colour scales used for each plot.

The declines in both northern and southern Basin are driven by significant declines in cool season (May–Oct) rainfall, in part of the uplands and slopes in the northern Basin, and almost in the entire southern Basin. Declines in cool season rainfall in parts of the southeastern southern Basin uplands is around $4 \text{ mm}\cdot\text{yr}^{-2}$, or 208 mm over 52 years. Trends in warm months rainfall show increases (but not statistically significant) in the southeastern southern Basin uplands and slopes, and scattered areas in the northern Basin. The analysis with updated data strengthens the notion that the dominance of cool season rainfall over warm season rainfall in the southern Basin has weakened (Whetton and Chiew, 2021). In addition, Dey et al. (2020) shows significant negative trends in longer duration rainfall events (>3 days) in uplands both in the northern and southern MDB. Also confirming findings for rainfall stations in the northern MDB in Chiew et al. (2022), declining rainfall in dry (cool months) season months in the northern MDB may reduce water availability as drier catchment conditions before wet season rains can amplify reductions in runoff

(Chiew, 2006). Rainfall characteristics for the entire MDB and the associated landforms is summarised in Table 2.

Rainfall anomalies for the landforms in the northern and southern Basins reflect the variability and the dominating dry conditions in the last two decades (Figure 4). In 2017/18–2019/20 rainfall anomalies were on average 30% (220 mm yr^{-1}) below mean annual rainfall in the northern MDB uplands, the runoff generating area of the northern Basin.

In the northern Basin, most years were below average from 2010/11 to 2019/20, and 2017/18–2019/20 had characteristics of a ‘flash drought’ (i.e., abnormally high temperatures, strong winds, increased solar radiation besides rainfall deficits) after the rapid decline of wetter than average conditions prevailing in 2016/17 (Nguyen et al., 2021). Much less is known about the drivers of dry periods in the northern Basin and if there is a similar non-stationary response beyond the ‘flash drought’ years, although research analysing climate drivers, such as the role of oceanic moisture sources also point to reductions in the cool season rainfall in 2017/18–2019 (Holgate et al., 2020; Taschetto et al., 2023).

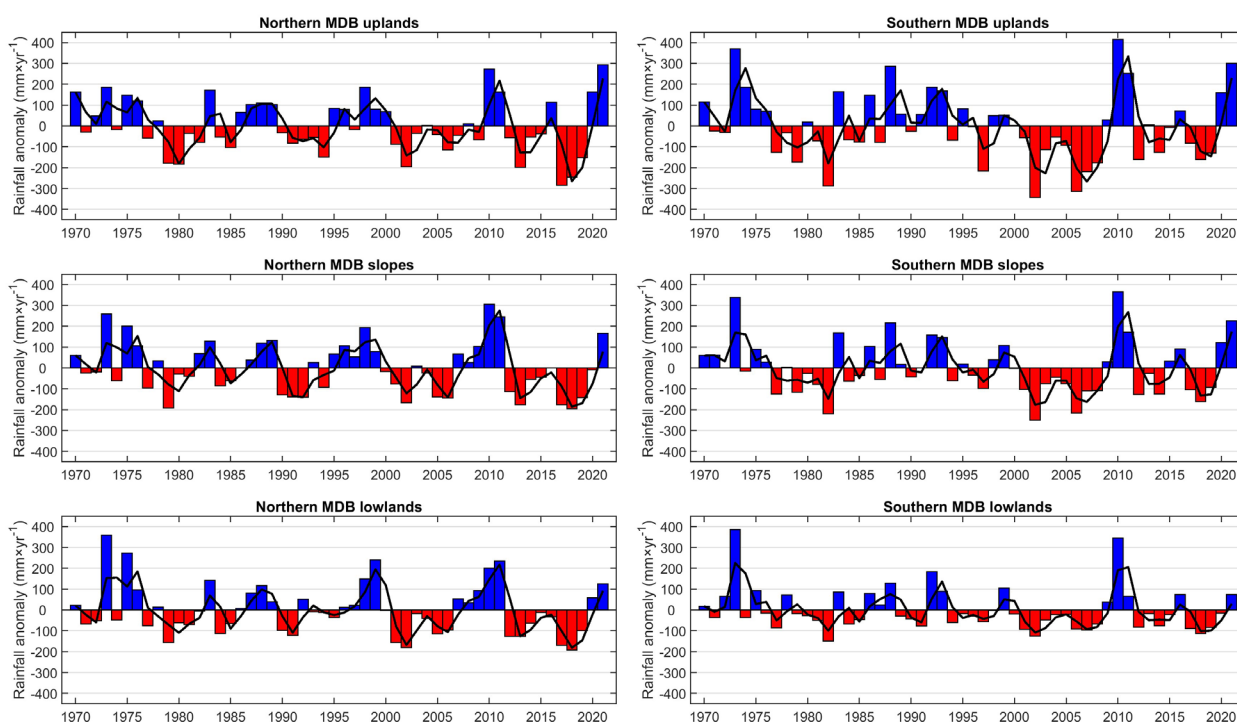


Figure 4. Annual (July to next June) Australian Gridded Climate Dataset (AGCD) rainfall anomalies for 1970/71–2021/22 anomalies averaged for landforms (each row) across the Murray–Darling Basin (MDBA). Anomalies based on the 1970/71–2021/22 baseline year. The left column shows averages for the northern Basin landforms, the right column shows averages for the southern Basin landforms.

The causality of the ‘Millennium drought’, i.e. multi-annual reduction in cool season rainfall, has been studied in detail, from seasonal and event perspectives (Gallant et al., 2012; Verdon-Kidd and Kiem, 2009), large scale drivers (King et al., 2014; Post et al., 2014; van Dijk et al., 2013) and resulting post-drought non-stationarity in southern Basin catchments (e.g., Fowler et al., 2022; Saft et al., 2016). The 2017/18–2019/20 drought, recent wet La Niña years and the twofold increased risk of an El Niño (<http://www.bom.gov.au/climate/enso/>, issued on 23 May) occurring

this year and the potential dry climate it may bring will provide more opportunities to assess non-stationarity in the northern Basin.

Table 2. Summary of rainfall characteristics in the Murray–Darling Basin (MDB) and associated landforms. Significant ($p < 0.1$) trends in bold. NMDBU=Northern MDB Uplands, NMDBS= Northern MDB Slopes, NMDBL= Northern MDB Lowlands. Similar nomenclature is used for the southern MDB (SMDB).

Landform	Annual (Jul-Jun)			Cool months (May-Oct)			Warm months (Nov-Apr)		
	Mean (mmy ⁻¹)	Coefficient of variation (%)	Trend (mmy ⁻²)	Mean (mmy ⁻¹)	Coefficient of variation (%)	Trend (mmy ⁻²)	Mean (mmy ⁻¹)	Coefficient of variation (%)	Trend (mmy ⁻²)
MDB	480	22	-1.34	218	32	-1.39	261	31	-0.30
NMDBU	721	18	-1.68	294	34	-1.43	426	22	-0.19
NMDBS	523	24	-1.71	184	41	-0.84	337	29	-0.60
NMDBL	392	31	-1.02	156	43	-0.75	235	45	-0.51
SMDBU	920	18	-1.87	513	27	-2.41	406	30	0.59
SMDBS	594	22	-1.60	325	30	-1.90	268	38	0.49
SMDBL	350	29	-1.04	189	34	-1.56	160	48	0.23

2.2 Evaporative demand

Evaporative demand, or potential evapotranspiration (PET) characterises the atmospheric demand for moisture from the land surface. PET is driven by climate variables such as temperature, solar radiation, relative humidity, and wind. If rainfall supply is low, soil moisture content is reduced through ET_a (Rodriguez-Iturbe et al., 1999), with dry catchment conditions inhibiting runoff production.

Budyko (1974) described long-term catchment balances with the supply-demand framework using the ratio of PET to rainfall (Figure 5), namely the dryness index. Dryness index < 1 denotes energy-limited environments (supply or rainfall exceeding demand or PET), whereas dryness index > 1 denotes water-limited environments. Around 98% of the MDB is considered water limited (Figure 5), with the areas mostly in the forested mountainous southeast being energy limited. Figure 5 (left panel) shows the Budyko curve, as water limitation increases then ET_a approaches rainfall hence runoff is small. Conversely, as water availability increases, then ET_a becomes closer to PET and more rainfall is converted into runoff (McVicar et al., 2012). In the MDB, rainfall is seasonal and variable, hence environments ‘straddle’ the threshold between the two limitations. According to McVicar et al. (2012) the areas where $0.75 \leq \text{dryness index} \leq 1.5$ can be considered ‘equitant’, which cover around 2.5% of the MDB. Increased PET can trigger a transition from energy limited to water limited environments, with concurrent reductions in runoff as less rainfall is partitioned into runoff.

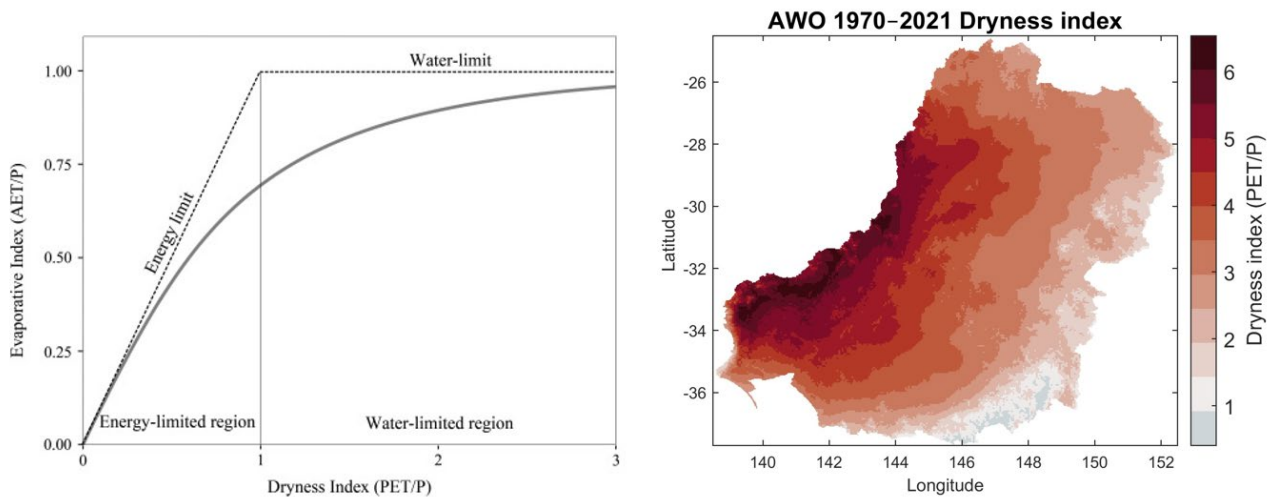


Figure 5. Budyko framework for annual water and energy balances (source: Trancoso et al. (2016)) and dryness index (PET/P) in the Murray–Darling Basin. AET=actual evapotranspiration, PET=potential evapotranspiration, P=rainfall.

Basin averaged mean annual PET (1970/71–2021/22) is $1,481 \text{ mmy}^{-1}$ (range $802\text{--}1,747 \text{ mmy}^{-1}$, Figure 6). Annual PET $<1,100 \text{ mmy}^{-1}$ occurs in the mountainous areas in the southeast, whereas PET $>1,400 \text{ mmy}^{-1}$ occurs in the northern basin slopes. Mean annual PET in the northern MDB is about $1,592 \text{ mmy}^{-1}$ (range $1,178\text{--}1,747 \text{ mmy}^{-1}$) and around $1,357 \text{ mmy}^{-1}$ (range $803\text{--}1,531 \text{ mmy}^{-1}$) in the southern Basin.

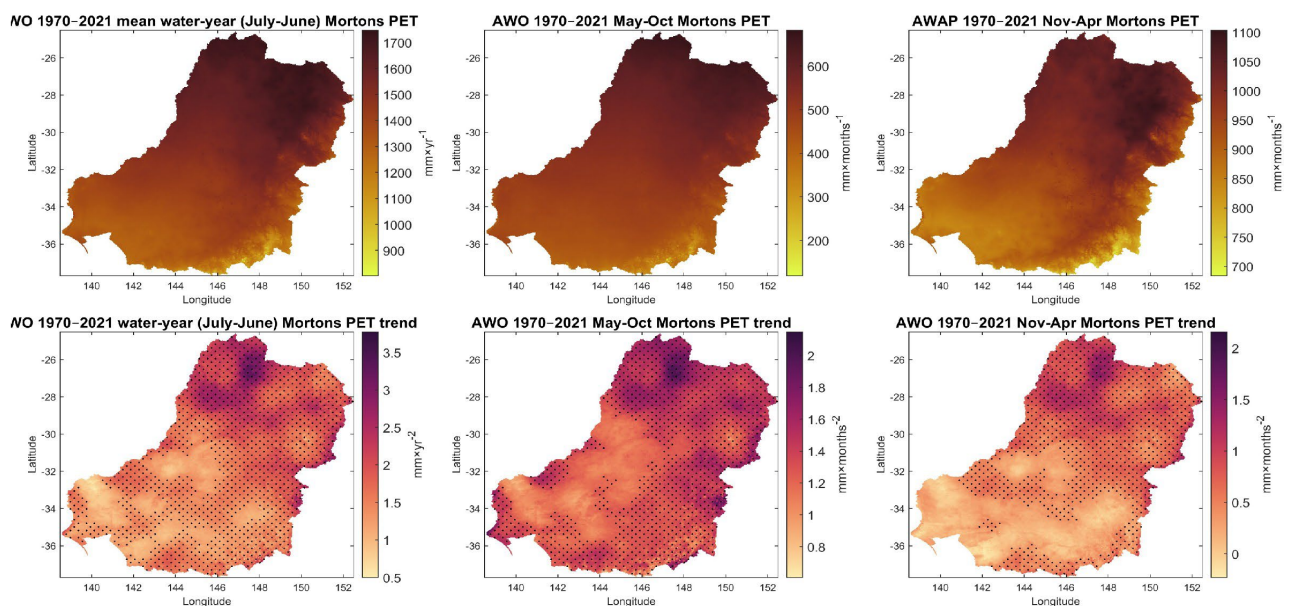


Figure 6. Spatial distribution of Australian Water Outlook (AWO) evaporative demand (or potential evapotranspiration, PET) and associated trends in the Murray–Darling Basin (MDBA). The first column shows mean annual (July to next June) PET, the middle column May to October PET (i.e., the cool months), and the third column November to next April PET (i.e., the warm months). The stipple (black dots) shows 0.05° pixels with significant trends ($p < 0.1$). Note the different colour scales used for each plot.

PET has significantly ($p < 0.1$) increased from 1970/71 to 2021/22 in most of the MDB (Figure 6), both during the cool months and warm months. The significant increase in annual PET in the northern Basin is of 1.65 mmy^{-2} , or 86 mm from 1970/71 to 2021/22. The significant increase in

the southern Basin is 0.90 mmy^{-2} , or 47mm from 1970/71 to 2021/22. In the cool and warm months, increases in most of both northern and southern MDB are significant. Temperature is the most important variable for PET in Australia (Guo et al., 2017) and it has been steadily increasing across the MDB, particularly since the 1950s (Whetton and Chiew, 2021). During the 2017/18–2019/20 drought, there were several maximum temperatures records in the northern Basin, coupled with clear skies and increased radiation (BoM, 2020). Table 3 summarises PET characteristics for the entire MDB and its landforms.

PET anomalies over the MDB landforms show the dominance of above average PET during the last 30 years. Anomalies after the below average years 2010/11 and 2011/12 and until 2020/21 generally exceeded 50 mmy^{-1} in the northern Basin landforms. Anomalies since 2020/21 were lower than average due to prevailing wet and cool La Niña conditions.

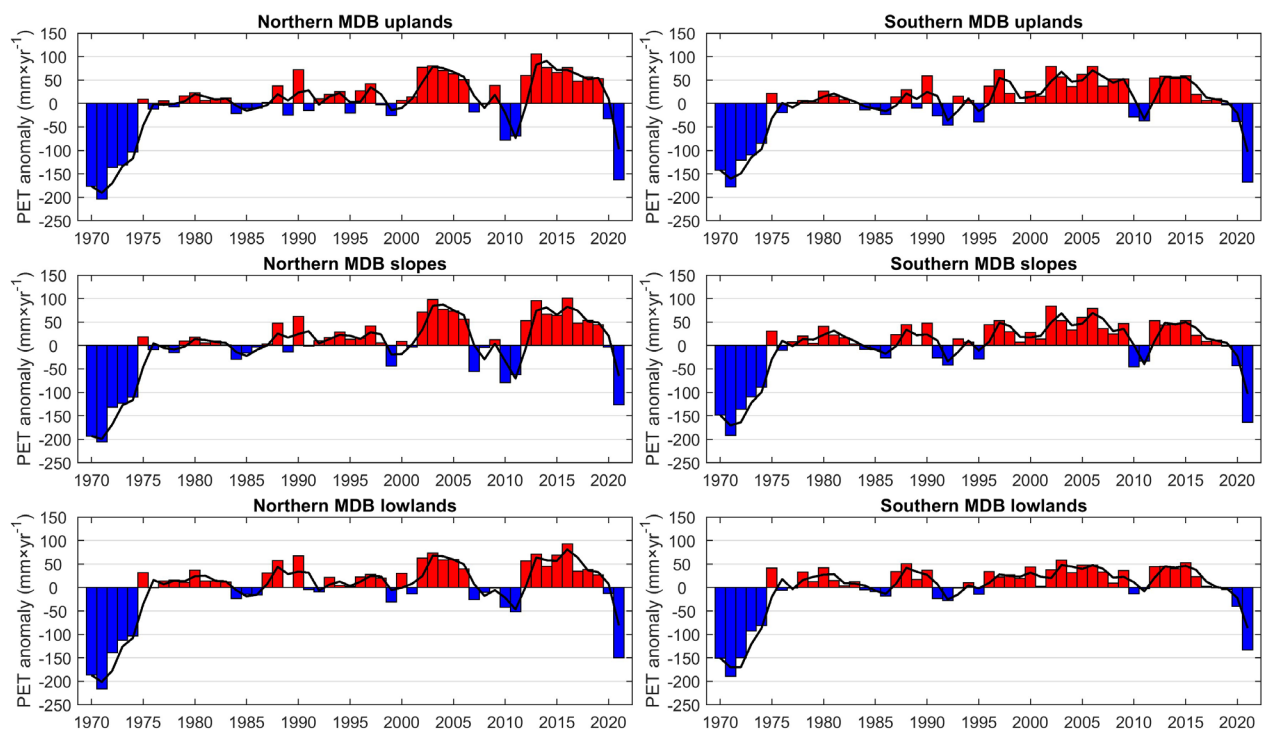


Figure 7. Annual (July to next June) Australian Water Outlook (AWO) evaporative demand (PET) anomalies for 1970/71–2021/22 averaged for landforms (each row) across the Murray–Darling Basin (MDBA). Anomalies based on the 1970/71–2021/22 baseline year. The left column shows averages for the northern Basin landforms, the right column shows averages for the southern Basin landforms.

PET plays a primary role in runoff generation (Trancoso et al., 2016) and its use can aid predicting droughts within a few weeks (Nguyen et al., 2021; Parker et al., 2021). The trends in Figure 6 show that PET is significantly increasing during wet seasons in both northern and southern MDB, which can exacerbate runoff decreases during long dry spells (Fowler et al., 2022).

Table 3. Summary of potential evapotranspiration (PET) characteristics in the Murray–Darling Basin (MDB) and associated landforms. Significant ($p<0.1$) trends in bold. NMDBU=Northern MDB Uplands, NMDBS= Northern MDB Slopes, NMDBL= Northern MDB Lowlands. Similar nomenclature is used for the southern MDB (SMDB).

Landform	Annual (Jul-Jun)			Cool months (May-Oct)			Warm months (Nov-Apr)		
	Mean (mmy ⁻¹)	Coefficient of variation (%)	Trend (mmy ⁻²)	Mean (mmy ⁻¹)	Coefficient of variation (%)	Trend (mmy ⁻²)	Mean (mmy ⁻¹)	Coefficient of variation (%)	Trend (mmy ⁻²)
MDB	1481	4	1.23	521	7	0.49	960	7	0.73
NMDBU	1496	5	1.84	536	8	0.74	960	8	1.11
NMDBS	1647	4	1.80	608	7	0.76	1038	7	1.15
NMDBL	1565	4	1.22	558	7	0.37	1007	7	0.86
SMDBU	1260	5	1.43	399	9	0.71	861	9	0.69
SMDBS	1391	4	1.04	453	8	0.53	938	8	0.54
SMDBL	1369	4	0.75	468	8	0.29	900	8	0.38

2.3 Runoff

The quantification and prediction of runoff is crucial for water resources management. In the mostly water limited MDB, runoff is the difference of the two much larger terms of the water balance, rainfall and ET_a . High spatiotemporal rainfall variability (Section 2.1) and water limited conditions in the MDB (Section 2.2) make the estimation of runoff difficult (Pilgrim et al., 1988). The sensitivity of runoff to climate inputs in the MDB is high, whereby proportional changes in mean annual runoff divided by the proportional changes in mean annual rainfall are higher than in many other basins globally (Chiew et al., 2006; Tang and Lettenmaier, 2012).

Estimates of runoff for the MDB are computed using the Australian Landscape Water Balance model version 7 (AWRA-L v7, Frost and Shokri, 2021). Various changes in the model's structure and calibration to capture water balance dynamics represented by the Gravity Recovery and Climate Experiment (GRACE) allowed a better representation (compared to the other national models trialled) of streamflow and its ephemerality or cease to flow characteristics (Frost et al., 2021). Basin averaged mean annual runoff (1970/71–2021/22) is about 30 mmy⁻¹, with high spatial (Figure 8) and temporal (Figure 9) variations. Annual runoff >1,000 mmy⁻¹ occur in the mountainous areas in the southeast, whereas runoff is <10 mmy⁻¹ in the Basin's west. The mean annual coefficient of temporal variation is 48%. Mean annual runoff in the northern MDB is about 25 mmy⁻¹ (range 0.7–347 mmy⁻¹) and around 34 mmy⁻¹ (range 0.1–1,164 mmy⁻¹) in the southern Basin. About 17 mm (68%) is generated in the northern basin during the warm months (November to March). Conversely, about 22 mm (65%) is generated in the southern Basin during the cool months (April to October). Table 3 summarises runoff characteristics for the entire MDB and its landforms.

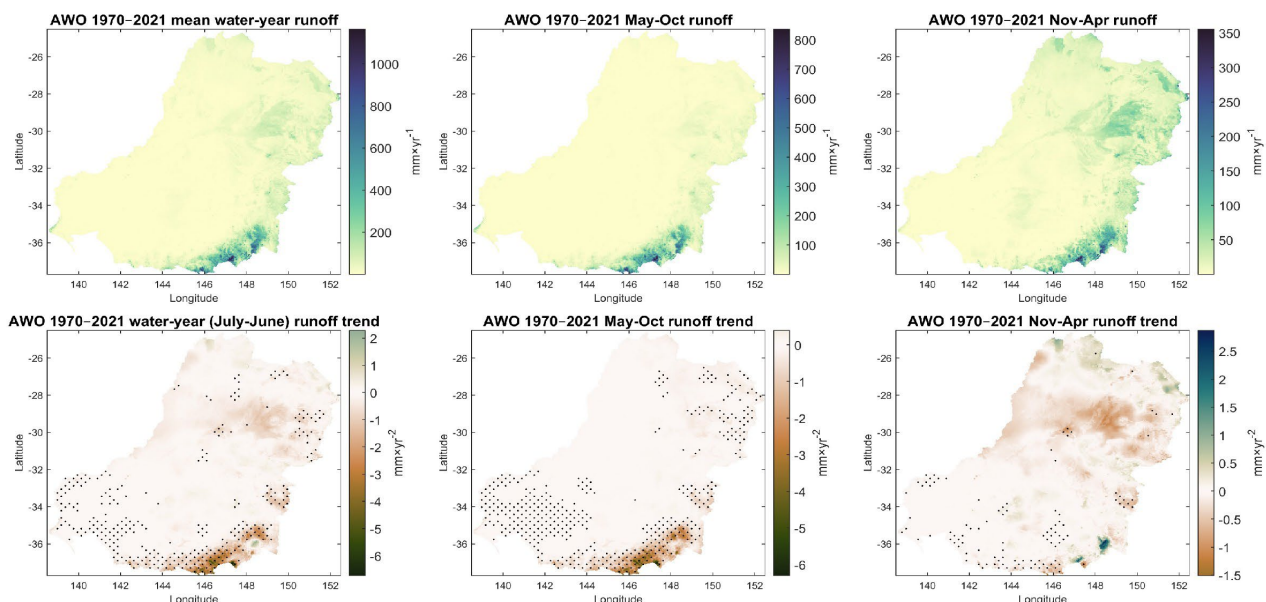


Figure 8. Spatial distribution of Australian Water Outlook (AWO) runoff and associated trends in the Murray–Darling Basin (MDBA). The first column shows mean annual (July to next June) runoff, the middle column May to October runoff (i.e., the cool months), and the third column November to next April runoff (i.e., the warm months). The stipple (black dots) shows 0.05° pixels with significant trends ($p < 0.1$). Note the different colour scales used for each plot.

Trends calculated for 1970/71–2021/22 show mostly declines in annual runoff (Figure 8), these are mostly located in the southern Basin. Some significant declines ($p < 0.1$) of around 6 mm \times yr $^{-2}$ are estimated in parts the southern Basin uplands, amounting to about 312 mm over 52 years. There are some areas with significant declining trends in the northern Basin upland with declines around 1 mm \times yr $^{-2}$. As for rainfall (Figure 3), the declines in the southern Basin are for both cool and warm months, whereas in the northern Basin the declines are mostly in the cool months (i.e., the dry season in the northern MDB). Interestingly, the increases in warm season rainfall in the southern MDB (Figure 3) have generally not translated into increases in warm season runoff (Figure 8) except for some limited areas in the mountainous areas of the southeast, as reduced cool season rainfall reduces runoff generating conditions.

Runoff anomalies showcase the variability and the dominating dry conditions in the last two decades (Figure 9). In 2017/18–2019/20 runoff anomalies were on average 58% (30 mm \times yr $^{-1}$) below mean annual runoff in the northern MDB uplands, the runoff generating area of the northern Basin. The below average conditions in the slopes in the northern Basin were similar, with average declines of 62% (14 mm \times yr $^{-1}$). In addition, all years from 2000/01 to 2009/10 had 20% below average anomalies in the northern MDB uplands.

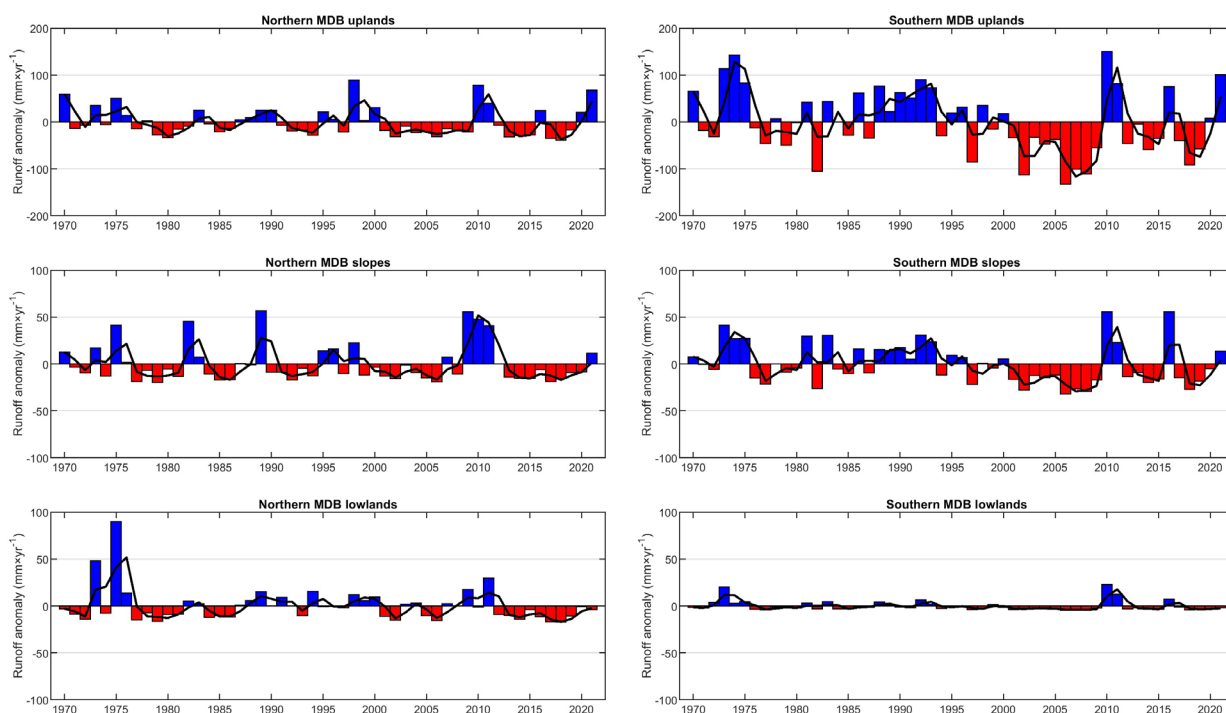


Figure 9. Annual (July to next June) Australian Water Outlook (AWO) runoff anomalies for 1970/71–2021/22 averaged for landforms (each row) across the Murray–Darling Basin (MDBA). Anomalies based on the 1970/71–2021/22 baseline year. The left column shows averages for the northern Basin landforms, the right column shows averages for the southern Basin landforms.

In the southern Basin uplands, 2006/07–2008/09 was 60% (114 mmy^{-1}) below average conditions. As pointed out by Potter et al. (2010) these dry periods in both northern and southern Basin uplands have a ratio of runoff reduction to rainfall reduction about 50% greater than the long term rainfall elasticity of runoff. These areas generate about 66% of basin flow and are most sensitive to changes in climatic conditions (Donohue et al., 2011). Besides changes in climate inputs, there are other catchment processes that influence the partition between rainfall and runoff, including changes in vegetation dynamics affecting ET_a , declines in groundwater storages, and irrigation and harvesting of runoff by small private dams (Fowler et al., 2022; Wentworth Group of Concerned Scientists, 2020). Some of these are explored in the next sections.

Table 4. Summary of runoff characteristics in the Murray–Darling Basin (MDB) and associated landforms. Significant ($p < 0.1$) trends in bold. NMDBU=Northern MDB Uplands, NMDBS= Northern MDB Slopes, NMDBL= Northern MDB Lowlands. Similar nomenclature is used for the southern MDB (SMDB).

Landform	Annual (July–June)			Cool months (May–Oct)			Warm months (Nov–Apr)		
	Mean (mmy^{-1})	Coefficient of variation (%)	Trend (mmy^{-2})	Mean (mmy^{-1})	Coefficient of variation (%)	Trend (mmy^{-2})	Mean (mmy^{-1})	Coefficient of variation (%)	Trend (mmy^{-2})
MDB	30	48	-0.21	15	59	-0.17	15	59	-0.03
NMDBU	51	60	-0.39	20	94	-0.20	30	94	-0.11
NMDBS	23	90	-0.08	5	189	-0.02	17	189	-0.01
NMDBL	19	96	-0.09	4	120	-0.03	14	120	-0.05
SMDBU	192	35	-1.29	131	46	-1.33	61	46	-0.20
SMDBS	39	55	-0.42	27	68	-0.36	12	68	-0.06
SMDBL	6	93	-0.05	3	89	-0.04	3	89	0.00

3 Vegetation

3.1 Actual evapotranspiration

Averaged across the MDB, 94% of rainfall becomes ET_a (Donohue et al., 2011). Under hotter and higher CO_2 conditions, vegetation response can either increase (through increased leaf area and forest biomass) or decrease water use (through a decrease in canopy conductance and higher water use efficiency). ET_a often declines under dry conditions due to reduced soil moisture supply, but can also increase due to evaporative demand and cause rapid depletion of water resources (Zhao et al., 2022). In the water limited MDB, an increase in ET_a can amplify runoff reductions.

Satellite-based ET_a models, which capture vegetation dynamics, are often only available since the 2000s. To assess variability and trends since 1970/71, the ERA5-Land (Muñoz-Sabater et al., 2021) reanalysis product – which includes a leaf area index (LAI) climatology from MODIS – is used in the ET_a analysis. Note that the use of MODIS monthly LAI climatology addresses monthly variability, but not inter-annual variability. It is planned that close to real time LAI will be included in the model (Muñoz-Sabater et al., 2021). A comparison of ERA-5 Land, the locally calibrated product CMRSET v2.2 (Guerschman et al., 2022) and PML v2 – a global product calibrated also with Australian eddy-covariance flux tower data (Zhang et al., 2019) – was undertaken in their overlapping period (2000/01–2019/20) and is shown in Appendix A. The results of the comparison indicate that ET_a from ERA5-Land is generally suitable to assess trends and variability, although its estimates vary from those of CMRSET, particularly during the wet 2010/11.

Basin averaged mean annual ET_a (1970/71–2021/22) is about 476 mmy^{-1} , with high spatial (Figure 10) and temporal (Figure 11) variations.

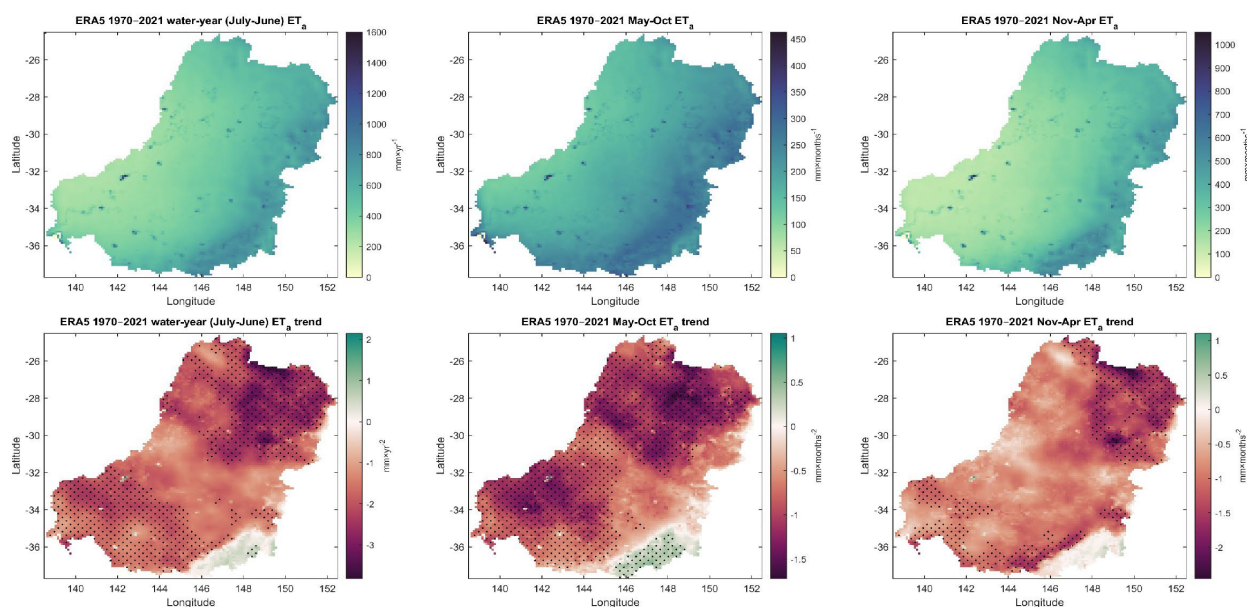


Figure 10. Spatial distribution of ERA5-Land actual evapotranspiration (ET_a) and associated trends in the Murray–Darling Basin (MDBA). The first column shows mean annual (July to next June) ET_a , the middle column May to October ET_a (i.e., the cool months), and the third column November to next April ET_a (i.e., the warm months). The stipple (black dots) shows 0.05° pixels with significant trends ($p < 0.1$). Note the different colour scales used for each plot.

Annual $ET_a > 1,000 \text{ mmy}^{-1}$ occurs in the east of the Basin, whereas $ET_a < 400 \text{ mmy}^{-1}$ happens in the Basin's west. The mean annual coefficient of temporal variation is 18%. Mean annual ET_a in the northern MDB is about 493 mmy^{-1} (range $258\text{--}1,106 \text{ mmy}^{-1}$) and around 456 mmy^{-1} (range $235\text{--}1,448 \text{ mmy}^{-1}$) in the southern Basin. Warm months (November to March) ET_a is 60% (298 mmy^{-1}) and 55% (253 mmy^{-1}) of annual ET_a in the northern and southern Basin, respectively. Table 5 summarises ET_a characteristics for the entire MDB and its landforms.

Trends calculated for 1970/71–2021/22 show declines in annual ET_a (Figure 10) except for the mountainous and largely forested southeast. Across the basin and annually, ET_a is declining significantly ($p < 0.1$) at 1.87 mmy^{-2} . Significant declines are present in most uplands and slopes in the northern Basins, and uplands, slopes, and lowlands in the south of the southern Basin. Some pixels with significant declining trends in the northern Basin uplands have declines $> 3 \text{ mmy}^{-2}$ or 156 mm over the 52 years. Declines in parts of the northern Basin uplands occur both in the cool and warm season months. On average annually, significant declines occur in all landforms in the northern Basin, whereas significant declines occur only on the southern Basin lowlands (Table 5).

ET_a anomalies over the northern MDB uplands in 2017/18–2019/20 were on average 35% (190 mmy^{-1}) below mean annual ET_a over the entire Basin, and 31% (171 mmy^{-1}) in the northern MDB slopes. Anomalies in the southern MDB uplands were lower on average during the same period but increasing in magnitude in the slopes and lowlands. Across the Basin, the last two decades have mostly been below average ET_a , with the exception of La Niña years in 2010/2011 and the following 2011/12, which had favourable rainfall and soil moisture conditions for ET_a production.

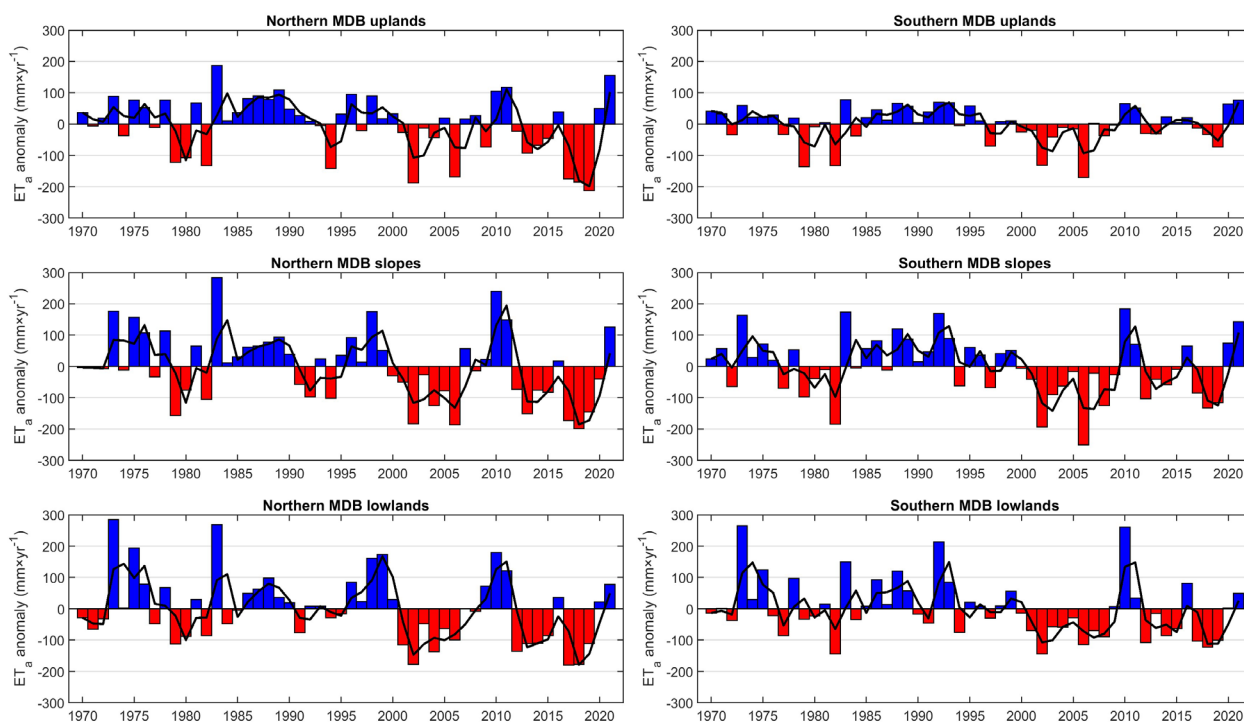


Figure 11. Annual (July to next June) ERA5-Land actual evapotranspiration (ET_a) anomalies for 1970/71–2021/22 averaged for landforms (each row) across the Murray–Darling Basin (MDBA). Anomalies based on the 1970/71–2021/22 baseline year. The left column shows averages for the northern Basin landforms, the right column shows averages for the southern Basin landforms.

It is of note that in 2017/18–2019/20, ET_a in the southern Basin uplands did not experience the same magnitude of negative anomalies as their northern counterpart. Notwithstanding

differences in rainfall anomalies in these landforms (see Figure 4), with larger decreases in the northern MDB uplands, the southern MDB uplands had on average a very modest decrease of 5% (39 mmy^{-1}), compared to 27% (190 mmy^{-1}) in the northern MDB uplands. These differences are likely related to the higher density of woody vegetation (i.e., forests) in energy limited areas in the southern MDB uplands (see Figure B.1., Lucas et al., 2019), whereas woody vegetation is of lower density in the northern MDB uplands and higher densities are confined to smaller areas (Figure B.1.). While trees are able to regulate water use during dry periods and have access to deeper soil water, herbaceous vegetation is more sensitive to higher radiation and/or temperature than woody vegetation, particularly in low rainfall areas (De Kauwe et al., 2017). Gardiya Weligamage et al. (2023) found similar small variations in ET_a in undisturbed and mostly forested catchments in Victoria during the Millennium Drought. ET_a is sensitive not only to changes in climate but also to land use changes such as deforestation or plantation forestry, and these changes may also be affecting ET_a in the northern Basin (Roderick and Farquhar, 2011).

Table 5. Summary of actual evapotranspiration (ET_a) characteristics in the Murray–Darling Basin (MDB) and associated landforms. Significant ($p < 0.1$) trends in bold. NMDBU=Northern MDB Uplands, NMDBS= Northern MDB Slopes, NMDBL= Northern MDB Lowlands. Similar nomenclature is used for the southern MDB (SMDB).

Landform	Annual (July-June)			Cool months (May-Oct)			Warm months (Nov-Apr)		
	Mean (mmy^{-1})	Coefficient of variation (%)	Trend (mmy^{-2})	Mean (mmy^{-1})	Coefficient of variation (%)	Trend (mmy^{-2})	Mean (mmy^{-1})	Coefficient of variation (%)	Trend (mmy^{-2})
MDB	476	19	-1.87	198	22	-1.02	278	22	-1.06
NMDBU	690	13	-1.66	260	16	-0.47	430	16	-1.19
NMDBS	508	22	-2.59	191	30	-1.24	316	30	-1.42
NMDBL	406	27	-1.75	172	35	-1.31	233	35	-0.71
SMDBU	734	8	-0.58	264	5	0.11	470	5	-0.62
SMDBS	607	16	-1.61	257	13	-0.41	350	13	-1.19
SMDBL	381	24	-1.81	183	23	-1.37	198	23	-0.83

It is noted that the forested area in the southeast MDB is experiencing significant reductions in wet season rainfall and a significant increase in PET and ET_a , with concurrent significant decreases in runoff. This is evidence of expected vegetation responses to increasing atmospheric CO_2 , including ‘greening’ with increased ET_a and decreased runoff (Ukkola et al., 2016). Simulations suggest climate change will bring further shifts towards ecosystem water limitation in current water-limited regions in the southern MDB (Denissen et al., 2022).

3.2 Vegetation phenology

Changes in vegetation ‘greening’ due to increases in CO_2 have been observed in shrubland ecosystems in Australia (Winkler et al., 2021) and catchments in the MDB (Ukkola et al., 2016). There are also areas within the MDB that have experienced ‘browning’ (Rifai et al., 2022). Figure 12 shows Leaf Area Index (LAI) and associated trends in the MDB for 2000/01–2021/22. Significant ($p < 0.1$) greening trends (e.g., positive LAI trends) are observed mostly in the southern Basin, in the southeast uplands and central lowlands. A few areas with significant greening trends are present in the northern MDB uplands and slopes, but overall, the northern MDB shows no high greening

nor browning trends. Note that the trends are estimated for the mostly drier than average last two decades, and some of the dynamics are impacted by bushfires, particularly in 2019/20.

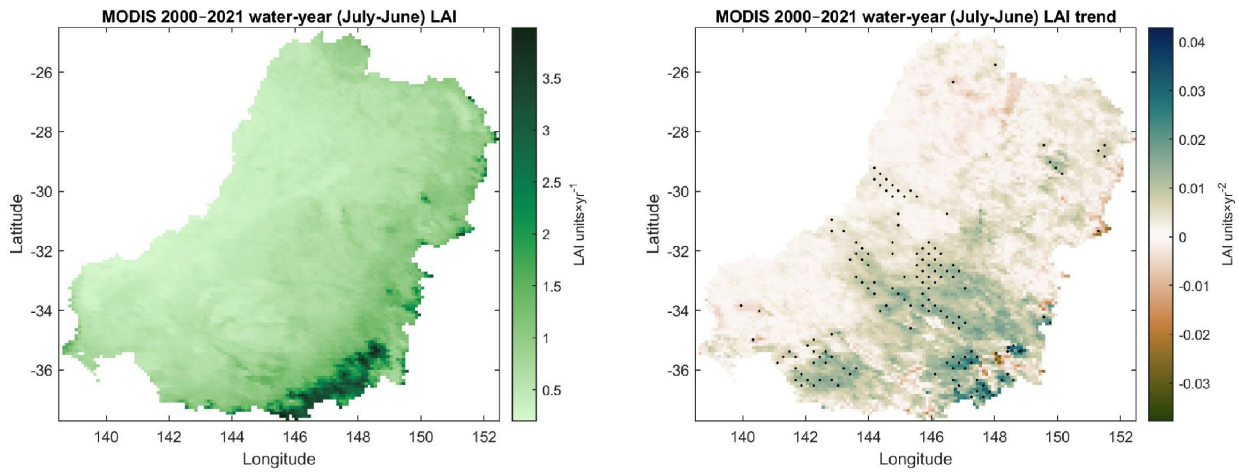


Figure 12. Spatial distribution of MODIS Leaf Area Index (LAI) and associated trends in the Murray–Darling Basin (MDBA). The stipple (black dots) shows 0.05° pixels with significant trends ($p < 0.1$).

LAI anomalies showcase differences in the northern and southern basin pertaining to drier than average periods. Relatively large (>0.2) negative anomalies during the Millennium Drought years in 2002/03–2008/09 occur in the southern Basin uplands and slopes. In contrast, relatively large anomalies in the northern Basin uplands occur in 2017/18–2019/20. This agrees with ET_a anomalies (Figure 11).

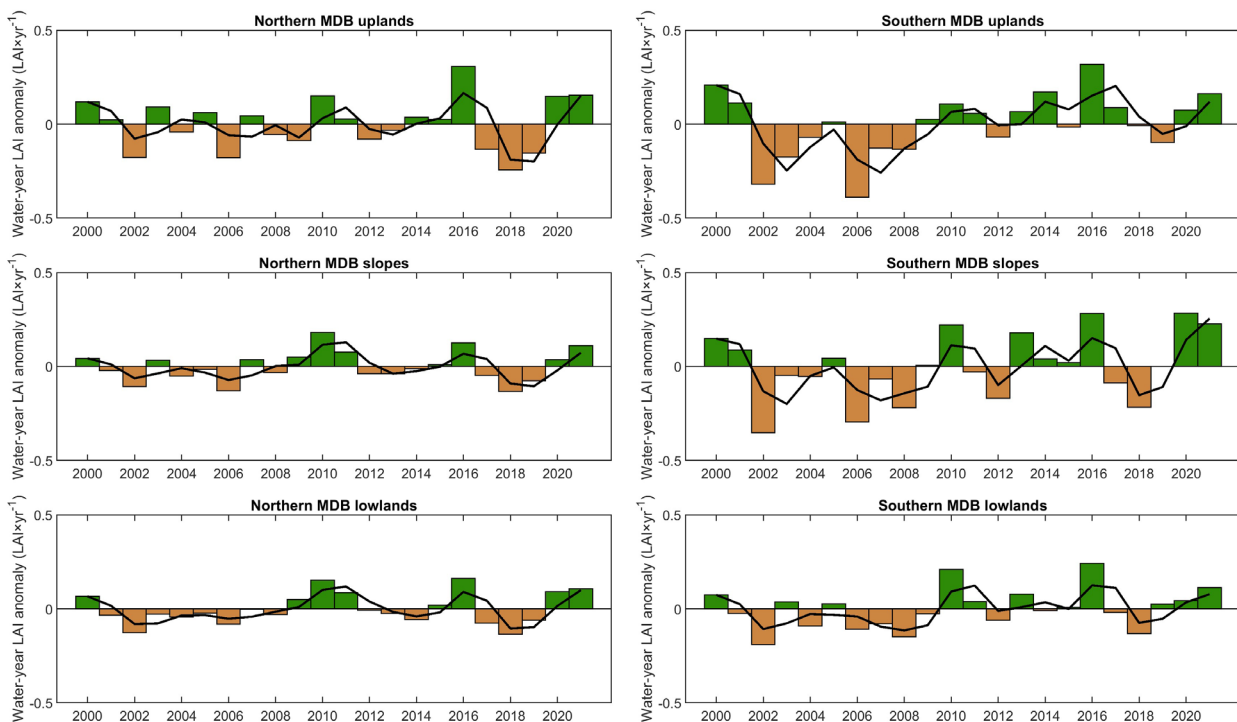


Figure 13. Annual (July to next June) MODIS Leaf Area Index (LAI) anomalies for 2000/01–2021/22 averaged for landforms (each row) across the Murray–Darling Basin (MDBA). Anomalies based on the 2000/01–2021/22 baseline year. The left column shows averages for the northern Basin landforms, the right column shows averages for the southern Basin landforms.

4 Groundwater

4.1 Groundwater level

Groundwater levels (i.e., depth to water table, DTW) can be a useful integrator of most hydrological processes occurring in the soil and land surface (rainfall, evapotranspiration, recharge, extractions and surface-groundwater interactions). Fu et al. (2022) analysed trends in annual mean/minimum/maximum DTW at selected 910 bores in eight alluvial systems in the MDB for 1971–2021. Figure 14 shows the bores and mean DTW trends for 524 bores in the northern Basin (Condamine-Balonne, Gwydir and Namoi). The bores were selected based on continuous data availability for each year during the study period.

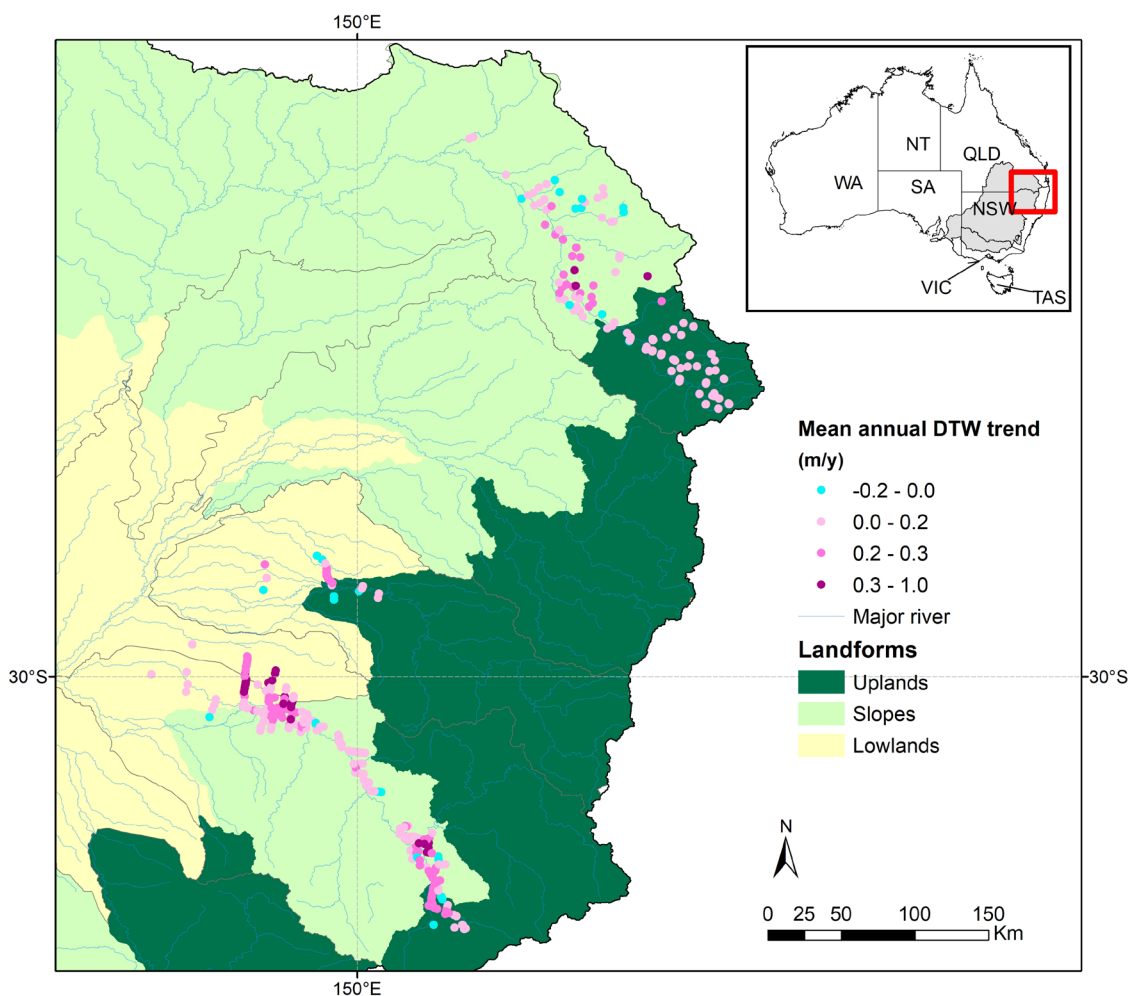


Figure 14. Spatial distribution of groundwater level trend (1971–2021) or Depth to Water Table (DTW) magnitude from 524 boreholes located in the northern Murray–Darling Basin (MDBA) and associated landforms (Fu et al., 2022).

The result of the analysis showcases mostly increasing trends in DTW (pink hues in Figure 14) attributable to reduction in groundwater recharge from reduced rainfall, and groundwater extraction for irrigation. Increases in DTW can result in the disconnection of the vadose zone from streams (Fowler et al., 2022), which is increasingly accepted as one of the main reasons for

observed catchment rainfall-runoff shifts (Chiew, 2006). A recent study by Crosbie et al. (2023) used bore data to assess changes in the direction of surface water-groundwater exchanges from 1970 to 2019 and found an increasing trend in losing reaches (i.e., streams contributing to groundwater) including in the northern Basin uplands (see Crosbie et al., 2023, and references therein).

4.2 Groundwater storage

The Gravity Recovery and Climate Experiment satellite mission (GRACE) provides estimates of variations of total terrestrial water storage at regional scales since 2002. GRACE data has been used to monitor declines in groundwater storage during the Millennium Drought (Leblanc et al., 2009). As for DTW data, GRACE variations integrate processes in the land surface. Figure 15 shows monthly storage anomalies of groundwater storage (GWS) averaged over the northern and southern MDB. GWS was obtained by subtracting the vegetation biomass water store, soil layers store, surface water store and snow store from the Global Land Data Assimilation System (GLDAS) 2.2 (Li et al., 2019). The baseline monthly anomaly was calculated for all months in the period 2003 to 2022. GRACE GWS shows the multiannual dry period during the Millennium drought in both northern and southern MDB, followed by the wet La Niña years 2010/11. The positive anomalies (or slightly negative) lasted 5 years, but in the case of the northern MDB steady drying since 2012/13 was followed by the declines in 2019/20 and onwards until 2021/22. Only the wet conditions in 2020/21 and subsequent years allowed the recovery of GWS. Dynamics in the southern MDB are different in that the recovery from the Millennium Drought included years with higher positive anomalies, followed by smaller declines in 2019/20 and onwards than in the northern Basin.

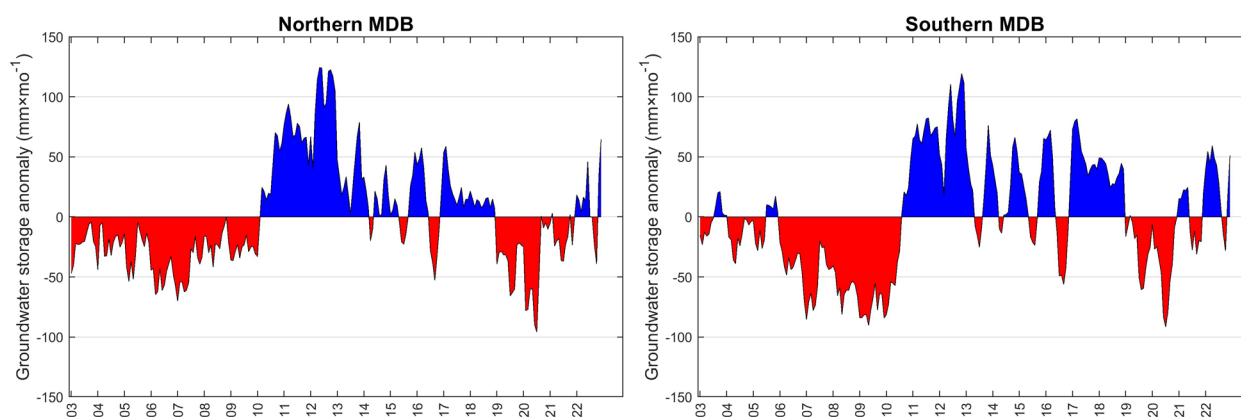


Figure 15. Monthly groundwater storage anomalies from the Gravity Recovery and Climate Experiment (GRACE) Mascon solutions for January 2003 to December 2022 averaged for landforms across the Murray–Darling Basin (MDBA). Anomalies based on the monthly 2003–2022 baseline month. The left column shows averages for the northern Basin, the right column shows averages for the southern Basin.

GRACE TWS data has been used in several studies in Australia besides monitoring of GWS. It has been used, inter alia, to evaluate representation of TWS in the AWRA model (van Dijk et al., 2011), assimilated to improve model deficiencies in simulating trends and seasonality of TWS (Schumacher et al., 2018), to evaluate rainfall-runoff model structural deficiencies (Fowler et al.,

2020) and to assess the role of water balance fluxes during the Millennium Drought (Gardiya Weligamage et al., 2023).

5 Anthropogenic changes

5.1 Irrigation

The northern MDB is an important cotton production area, using ~1,835 GL of water in 2017/18 (Goesch et al., 2020). The area equipped for irrigation (or irrigable areas, i.e., areas that have infrastructure to irrigate crops) in the northern MDB is ~10,000 km² (ABARES, 2021).

CMRSET Landsat V2.2 monthly ET_a minus rainfall (in volume units of GL) estimates from irrigable areas in the MDB (~35,200 km²) were aggregated to annual (i.e., water year from July to next June) and compared to surface water and groundwater take (Figure 16) from the MDBA (2022). Surface water take include extractions regulated rivers, watercourses and floodplain harvesting (see Figure 4-2 in MDBA, 2022). Besides extractions for irrigation, groundwater take also includes water for town water supply, and extraction to manage water table and salinity levels (Figure 4-3 in MDBA, 2022). ET_a minus rainfall provides a proxy of irrigation water use by vegetation (Bretreger et al., 2020; Bretreger et al., 2022; Peña Arancibia et al., 2021) in irrigated paddocks, although the estimates in Figure 16 all irrigable areas are included. Figure 16 highlights the similar magnitude in ET_a minus rainfall and water take, notwithstanding the methodological differences between both metrics. Generally, conveyance and application efficiencies mean that water take should be higher than ET_a minus rainfall if no other sources (like groundwater) of water are available. During dry years groundwater becomes more relevant and in the case of the northern Basin, there is also water stored in large (>100 ML) on-farm storages. The total capacity of on-farm storages in northern MDB is about 3,000 GL, and water stored therein can compensate shortfalls during dry years.

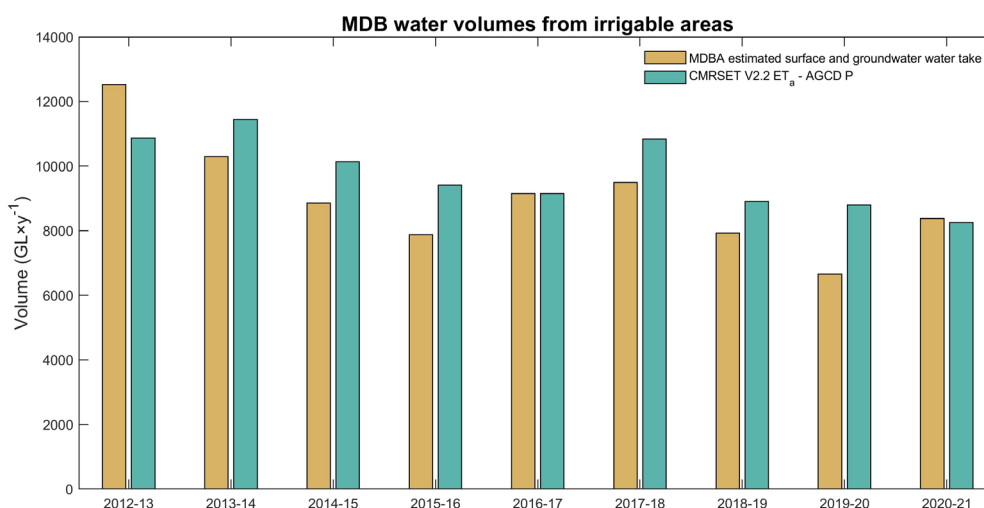


Figure 16. Comparison of annual Murray–Darling Basin (MDB) estimated bulk water take (brown bars, MDBA, 2022) against CMRSET V2.2 averaged actual evapotranspiration (ET_a) minus rainfall (from AGCD) (ET_a-P, green bars). Irrigable areas correspond to the entire MDB.

Figure 17 shows ET_a minus rainfall in 9 irrigation areas (IAs) in the northern MDB, except for the Darling Downs IA, the IAs are located in semi-arid areas in the northern MDB, hence most agricultural production is irrigated during the summer months (except for very wet years). The proxy of water use during the Millennium Drought and the dry 2017/19 to 2019/20 period showcases that water use was relatively sustained. It is likely that irrigated areas reduced their areal extension during dry years (as indicated by reductions in production, ABARES, 2019) with application rates increasing due to low soil moisture conditions.

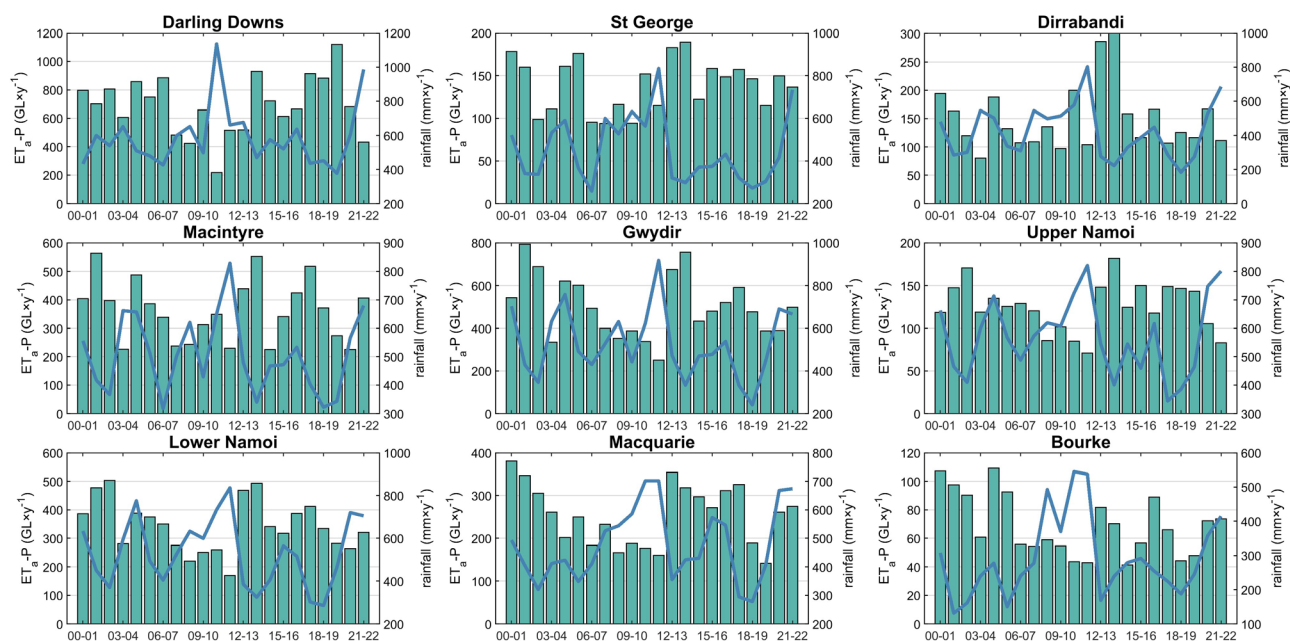


Figure 17. CMRSET V2.2 averaged actual evapotranspiration (ET_a) minus rainfall (from AGCD) (ET_a-P , green bars) and mean annual rainfall (blue line) for selected irrigable areas across the northern Murray–Darling Basin (see Figure 1).

Estimates of irrigation water use can be refined by using crop phenologies extracted from satellite-borne ‘greenness’ data (like LAI, see Section 3.2) and estimated areas that are actually irrigated (Peña-Arancibia et al., 2014). Similarly, hydrologic models can be used to assess provenance (e.g., surface water or groundwater) of water used in irrigation (Peña-Arancibia et al., 2016). These estimates can be used to improve estimates of water take in areas where water extraction metering is absent or prone to large errors.

5.2 Farm dams

Farm dams are an adaptation to climate variability, as they provide water during dry periods for irrigation, stock demand and domestic uses when surface water or reticulated water is not available. Individual farm dams have a relatively small impact on catchment water resources, but collectively they can reduce mean annual catchment streamflow, particularly during dry years (Habets et al., 2018; Morden et al., 2022).

The Malerba et al. (2021) dataset provides the spatial location of >1.7 million farm dams across Australia. This dataset was clipped for the MDB and volume characteristics were obtained using surface area-volume relationships established for 588 farm dams (Malerba et al., 2021). A recent

study by Peña-Arancibia et al. (under review) estimated growth rates in farm dam volume across the MDB using Landsat reflectance data timeseries (1986–2020) to detect presence of water in the farm dam for the first time, hence its commissioning year. These results were used here to report growth (in volumetric density, GLkm⁻²) across MDB landforms. Figure 18 shows total growth density across MDB landforms, which for all landforms has a loosely logarithmic growth. Fast growth rates ($\geq 10\%$) from 1986 to 1990 are likely unrealistic because an unknown number of farm dams would have been present in the landscape before the availability of Landsat imagery (around 1986) and are not shown here. Growth after 2010 generally tapers off for all landforms.

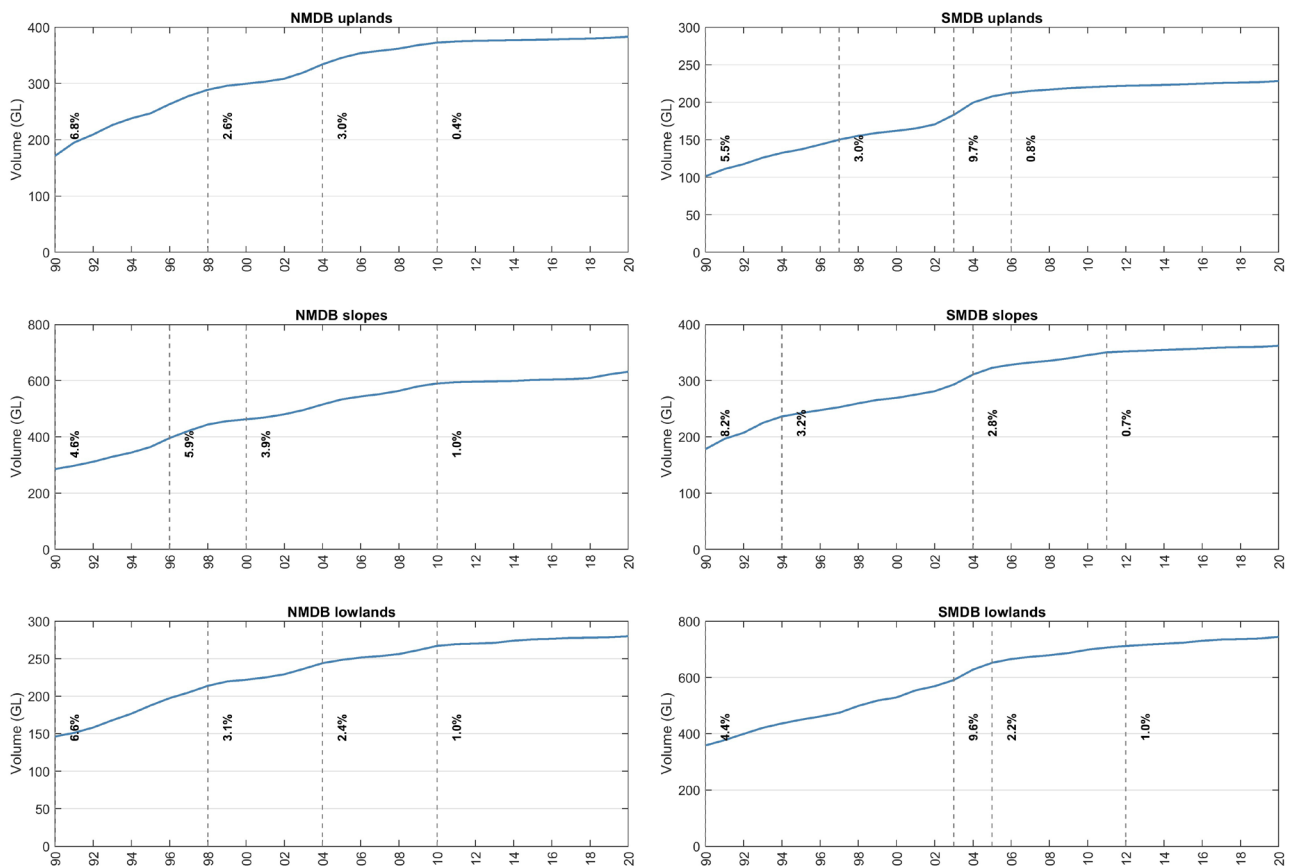


Figure 18. Annual timeseries (1986–2020) of aggregated farm dam volume density (in GLkm⁻²) for landforms in the Murray–Darling Basin. The left column shows averages for the northern Basin, the right column shows averages for the southern Basin. Horizontal black dashed lines indicate years were the slope and intercept of a linear regression fitted to the data changes abruptly. The rates of change for each segment are annotated next to each line and indicated in percentages.

The total farm dam storage volume across the MDB is 2,630 GL, with 1,284 and 1,346 in the northern MDB and southern MDB, respectively.

Figure 19 shows annual growth rates (in percentage) for all MDB landforms. After the fast growth in the 1990s, growth accelerated again during the Millennium Drought. This behaviour is not observed in the recent low rainfall years from 2017/18 to 2019/20.

The effects of farm dams on runoff reductions, which are mostly greatest on the low flows and during low flow months (Robertson et al., forthcoming), can be compounded due to the expected reduction in rainfall in parts of the MDB, particularly in the southern Basin (Whetton and Chiew,

2021), and the transition to more water limited conditions (Denissen et al., 2022; Ukkola et al., 2016).

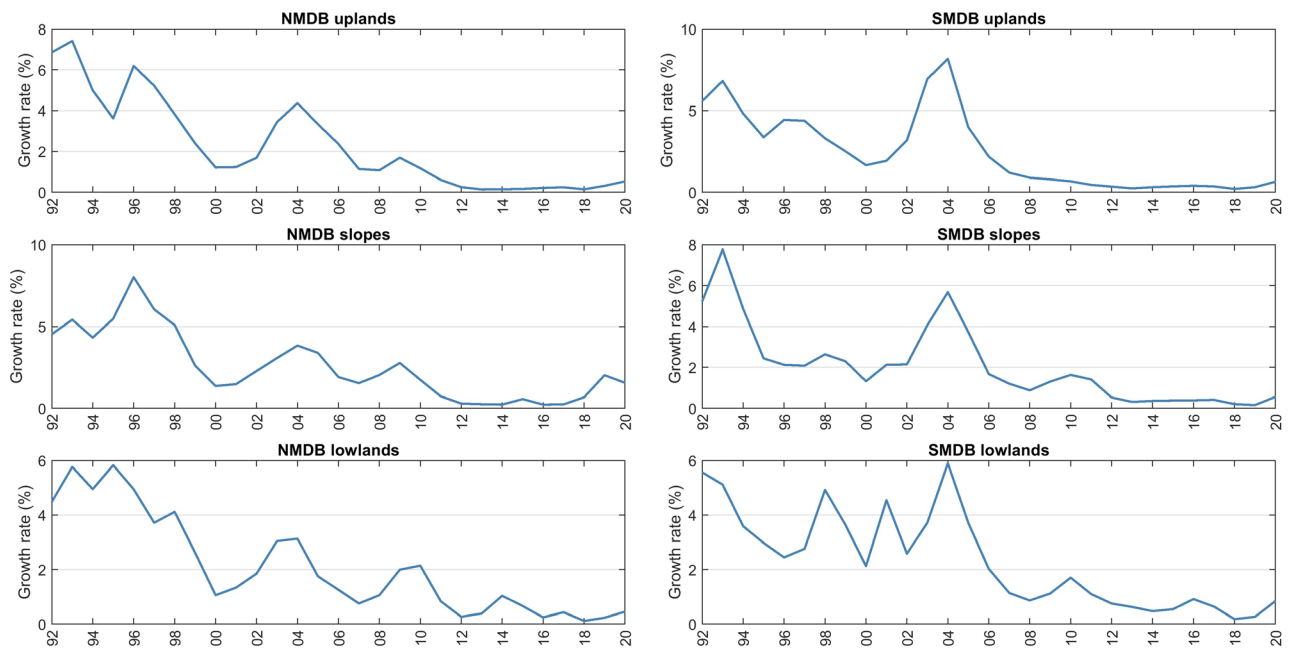


Figure 19. Annual timeseries (1992–2020) of aggregated farm dam growth rate (in percentage) for landforms in the Murray–Darling Basin. The left column shows averages for the northern Basin, the right column shows averages for the southern Basin.

6 Summary and recommendations

6.1 Summary

Climate in the last three decades in the Murray–Darling Basin (MDB) has been characterised by multiannual periods of drier than average conditions followed by wetter than average conditions that last for one to three years. During long dry periods, the rainfall-runoff elasticity characteristic of the MDB further reduces annual runoff generated from the same amount of annual rainfall.

This report analysed climate and catchment processes that have an impact on runoff across the MDB, with a focus on factors that can modify hydroclimate characteristics and dominant hydrological processes (i.e., ‘hydrologic non-stationarity’). The present analysis, to be followed next year by more comprehensive evaluation and modelling, primarily focuses on trends and variability at the annual scale (i.e., hydrological year from July to next June, hereafter referred to as annual) generally from 1970/71 to 2021/22, therefore updating previous analyses performed by the MDBA and Basin State agencies. The analysis of annual time series is employed to demonstrate key shifts in magnitudes and variability, both in time and space. To summarise the results, the MDB is disaggregated into uplands (runoff generating areas), slopes, and lowlands (with floodplains). The following climate and catchment processes have been analysed: (i) hydroclimate (rainfall, evaporative demand, runoff, groundwater), (ii) landscape dynamics (actual evapotranspiration (ET_a), vegetation, groundwater storage) and (iii) anthropogenic impacts including irrigation water use and farm dams.

The key findings are:

- Rainfall has declined over most of the MDB, the decline is statistically significant ($p < 0.1$) in parts of the northern and southern Basin uplands over the 52-year period (1970/71–2021/22), the areas that generate most of the Basin’s runoff. The decline has been dominated by reductions in cool season (May to Oct) rainfall. The significant decline in the uplands of the southern Basin was -2.41 mmy^{-2} and in the northern Basin uplands was -1.43 mmy^{-2} . There are increasing but not statistically significant rainfall trends during the warm months, mainly in the southern Basin, indicating an ongoing shift away from winter dominated rainfall as has been reported in the literature. The 1997–2009 ‘Millennium drought’ had lower than average rainfall in the southern Basin than in the northern Basin, but the following 2010/11 wet La Niña period had greater than average rainfall in the southern Basin than in the northern Basin. Conversely, the dry period from 2017/18 to 2019/20 in the northern Basin uplands had the lowest consecutive three-year period rainfall since 1970/71.
- Evaporative demand throughout the year has significantly increased across the MDB since 1970/71. The increase in PET is largely due to the increase in temperature. On average, the increases in PET are statistically significant for all landforms and cool and warm months in the northern MDB, whereas the increase is significant in both cool and warm months in the southern Basin uplands. Overall, the significant increase in the northern Basin was 1.62 mmy^{-2} and in the southern Basin was 1.07 mmy^{-2} . Significant increases, particularly during cool months, can compound decreases in rainfall and amplify decreases in runoff. In addition, the

multiannual above average evaporative demand from 2002/03 to 2019/20 (with few years slightly below average until the recent La Niña years) has been the highest since 1970/71, and higher for the northern Basin than the southern Basin.

- Runoff has mostly declined over the MDB, with significant annual declines mainly in the southern Basin uplands and slopes, and some areas of the northern Basin uplands. The annual declines are mainly caused by significant cool season declines. Overall, the statistically significant decrease in the northern Basin was -0.12 mmy^{-2} and in the southern Basin was -0.26 mmy^{-2} . Runoff anomalies highlight the high variability and the dominating dry conditions in the last two decades, with the highest multiannual below average conditions during the Millennium Drought in the southern Basin since 1970/71. Runoff was below average almost continuously from 2013/14 to 2019/20 in both northern and southern MDB, except for the wetter than average year 2016/17.
- Actual evapotranspiration (ET_a) has significant annual declines across the MDB, except the densely forested areas of the southern MDB uplands. The ET_a increase in the densely forested areas is statistically significant in the cool season (May to Oct). Significant declines during the warm season (Nov to Apr) occur mainly in the northern Basin uplands, and parts of the slopes and lowlands in the southern MDB. Overall, the statistically significant decrease in ET_a in the northern Basin was -2.10 mmy^{-1} and in the southern Basin was -1.67 mmy^{-1} . ET_a anomalies over the northern MDB uplands in 2017/18–2019/20 were the lowest since 1970/71. The results for ET_a , and associated results on rainfall, evaporative demand and runoff, suggest that parts of the Basin are shifting more towards ecosystem water limitation, including the energy limited areas in the southern MDB uplands.
- In terms of Leaf Area Index (LAI), the southern Basin, southeast uplands, and central lowlands exhibit noticeable 'greening' trends (i.e., positive LAI trends). In contrast, the overall trend in the northern MDB does not indicate substantial increases or decreases in vegetation LAI changes.
- In terms of groundwater, the analysis primarily indicates an increasing trend in depth to groundwater level in the northern valleys assessed (Condamine-Balonne, Gwydir and Namoi). These trends can be attributed to reduction in groundwater recharge from reduced rainfall and groundwater extraction for irrigation purposes. The increase in groundwater depth can lead to the separation of the vadose zone from streams, an occurrence increasingly acknowledged as a key factor contributing to changes in catchment rainfall-runoff patterns.
- Analysis of the GRACE Groundwater Storage (GWS) anomalies reveals a prolonged dry spell lasting multiple years during the Millennium Drought, affecting both the northern and southern MDB. This was followed by wetter conditions during the La Niña years of 2010/11. The positive anomalies, or slightly negative ones, persisted for five years after. However, in the northern MDB, a consistent drying trend emerged from 2012/13, which was further exacerbated by declines observed from 2019/20 until 2021/22. Only the wet conditions experienced in 2020/21 and subsequent years facilitated the recovery of GWS. The dynamics in the southern MDB differ in that the recuperation from the Millennium Drought included years with higher positive anomalies, followed by smaller declines from 2019/20 onwards compared to the northern Basin.

- The remote sensing proxy for irrigation water use in the northern Basin irrigated areas showed relatively modest changes in water use during the Millennium Drought and the dry period from 2017/19 to 2019/20. It is likely that irrigated agriculture experienced a reduction in their surface area during the dry years, as evidenced by declines in production. This may be due to increase in application rates to compensate for the low soil moisture conditions.
- In terms of farm dams, the analysis showed growth across MDB landforms, with fast growth rates during the 1990s and during the Millennium Drought. Growth has tapered off since 2010. The total farm dam storage volume across the MDB is 2,630 GL, with 1,284 GL and 1,346 GL in the northern MDB and southern MDB, respectively. The effects of farm dams on runoff reductions, which are greatest on low flows and during low flow months, can be compounded due to the expected reduction in rainfall in parts of the MDB, particularly in the southern Basin and the transition to more water limited conditions.

6.2 Recommendations

The analysis reported here from the first year of this study, performed at the annual scale, highlighted the magnitude, trend and variability of key hydrological variables across the Murray–Darling Basin and its landforms, both of natural and anthropogenic nature.

The second year of this study will conduct more detailed assessments to describe, quantify and model the reduction in catchment runoff caused by changes in climatic and landscape characteristics. Some of the analysis and modelling that will be explored are summarised below.

- Rainfall, evaporative demand and actual evapotranspiration data will be extended to the 1950s to provide more detailed insights on how changes in climate are affecting seasonality, intensities, and spatial patterns. Sequences of years with below average rainfall will be compared to recent dry periods and changes in seasonality and other rainfall characteristics (and associated weather systems) that are important for runoff generation will be assessed (Fu et al., 2023; Potter et al., 2010).
- Many studies (Chiew, 2006; Peterson et al., 2021; Saft et al., 2016) have used streamflow in unimpaired catchments, particularly in the southern MDB and Victoria, to assess the effects of long dry periods and non-stationarity on rainfall-runoff relationship. Some studies (Ajami et al., 2017; Deb et al., 2019) suggest that endogenous catchment characteristics (vegetation, slope, groundwater table) can be equally important in explaining shifts in the rainfall-runoff relation. Therefore, the logical step forward is to perform similar analyses in a set of catchments in the northern basins with curated streamflow data spanning 40 or more years. Attribution studies and machine learning can be used to assess the importance of endogenous characteristics and climate changes.
- Irrigation water use and water storage in large on-farm storages (i.e., water diversions) can also be better quantified by identifying irrigated areas (Peña-Arancibia et al., 2014) and water volumes in ring tanks using recent remote sensing radar data (Biancamaria et al., 2016) and on-farm storage modelling (Fuentes et al., 2021).
- The hypothesised causality will also be explored through hydrological modelling. This will include falsifying existing models as well as incorporating new dominant process

representation in the models. The use of more robust calibration strategies and datasets beyond streamflow (e.g., ET_a , GWS, LAI) to constrain model calibration will also be explored.

Appendix A Evaluation of alternative actual evapotranspiration models

This section shows a comparison between the three ET_a datasets used in this study. Figure A.1. shows the mean annual ET_a for ERA5-Land, PML V2 and CMRSET V2.2, showcasing similar spatial patterns and magnitudes.

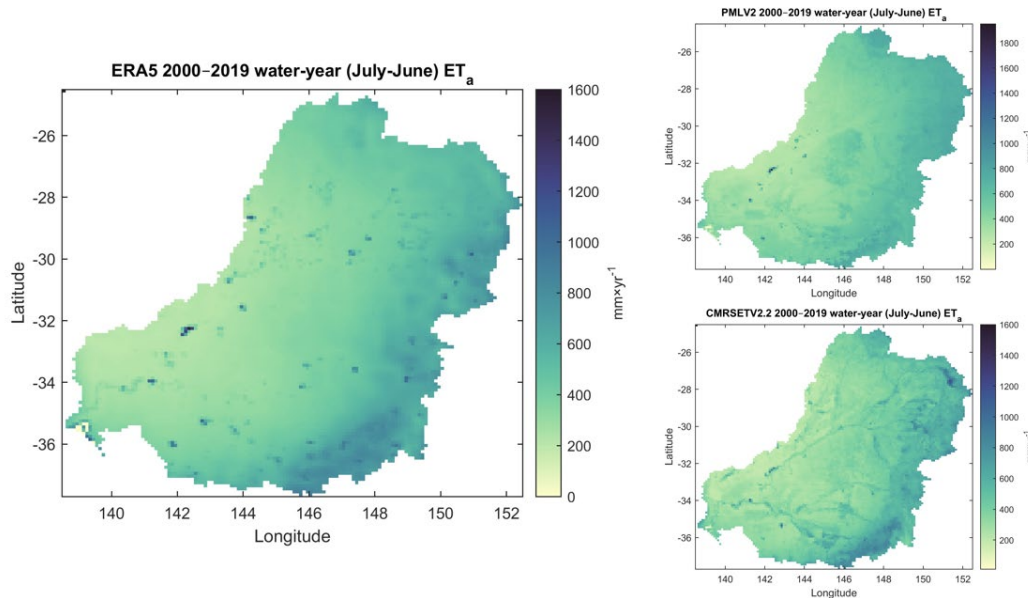


Figure A.1 Comparison of actual evapotranspiration (ET_a) products in the MDB

Figure A.2. shows a scatterplot between daily ET_a from the aforementioned products against 29 flux tower ET_a data across Australia (Beringer et al., 2017). In all products correlations are high (>0.8) and root mean squared error (RMSE) are low ($<0.7 \text{ mm} \times \text{day}^{-1}$).

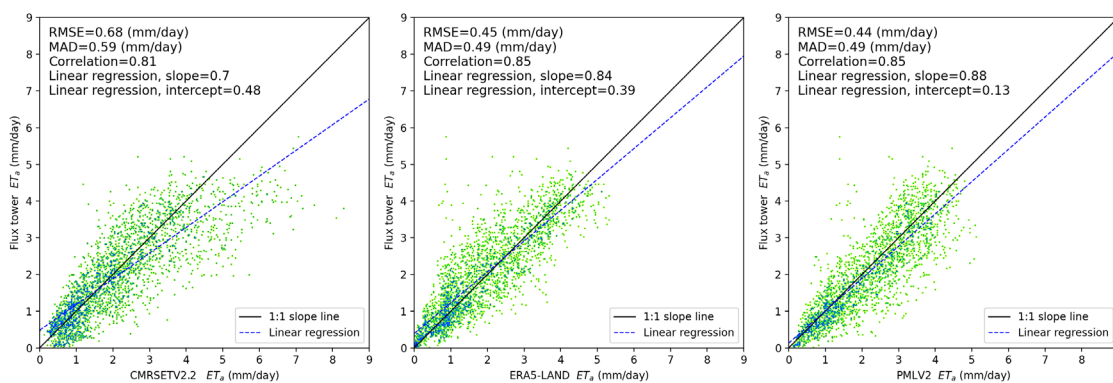


Figure A.2 Comparison of actual evapotranspiration (ET_a) models against flux tower ET_a data (left panel, CMRSET V2.2, middle ERA5-Land, right PML V2). Each plot shows the 1:1 line (black) and the best-fit linear regression line (blue). Goodness-of-fit statistics including the root mean squared error (RMSE), mean absolute difference (MAD), correlation and best-fit linear regression coefficients.

Figure A.3. shows timeseries of the different products averaged over MDB landforms. In the overlapping period (2000 to 2020) ERA5-Land and CMRSET V2.2 generally agree well in

magnitudes and temporal patterns, except for the wet 2010/11, in which CMRSET estimates are considerably lower.

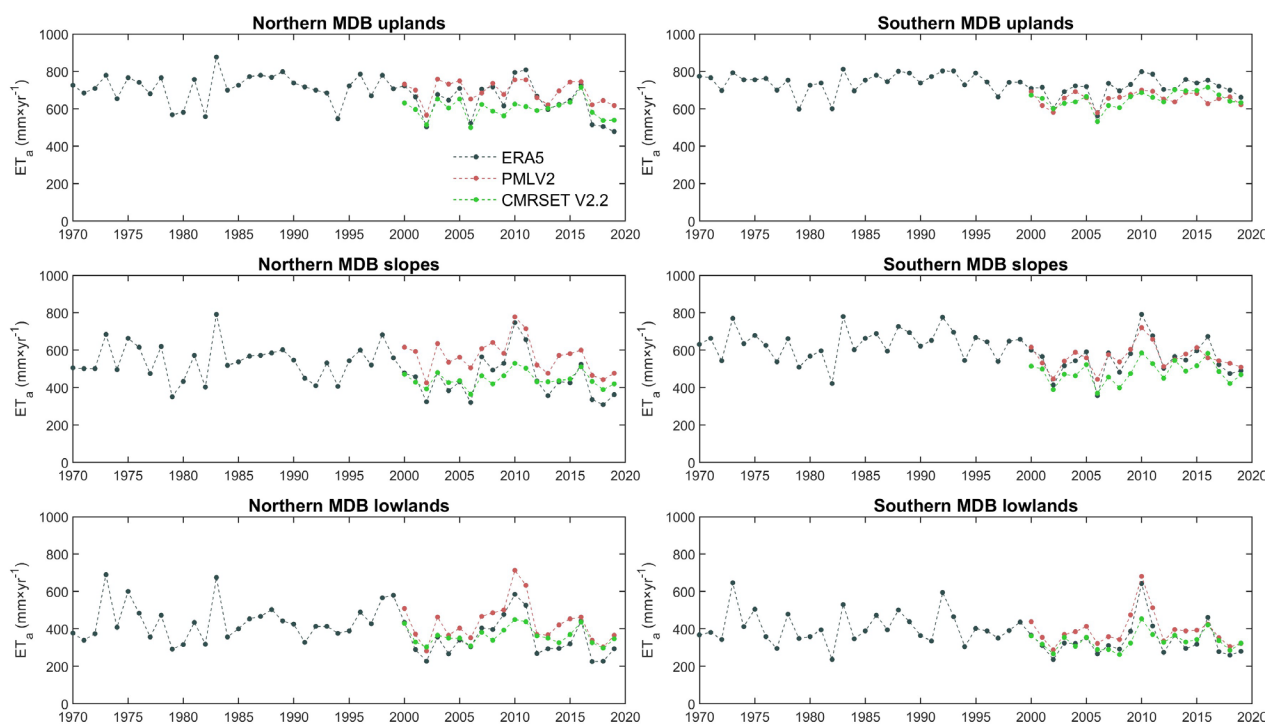


Figure A.3 Comparison of actual evapotranspiration (ET_a) timeseries averaged for landforms across the Murray–Darling Basin (MDBA).

Appendix B Other ancillary data

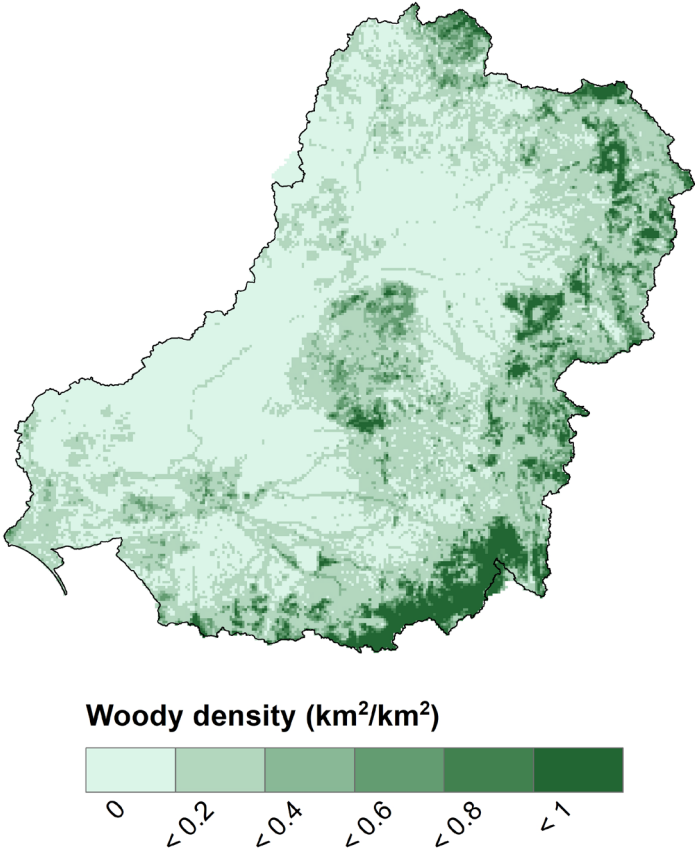


Figure B.1. Woody vegetation density c.a. 2019. Data from DEA Landcover (<https://www.dea.ga.gov.au/products/dea-land-cover>, accessed May 2023). Woody density is calculated on 5 km × 5km grid using 30 m maps of woody vegetation.

References

- ABARES, 2019. Australian crop report No. 192, Australian Bureau of Agricultural and Resource Economics and Sciences, pp. 29.
https://www.agriculture.gov.au/sites/default/files/documents/austcroprrt20191203_v1.0.0.pdf, last access: May 2023.
- ABARES, 2021. Catchment Scale Land Use of Australia – Update December 2020, Australian Bureau of Agricultural and Resource Economics and Sciences, Canberra, Australia.
<https://www.agriculture.gov.au/abares/aclump/catchment-scale-land-use-of-australia-update-december-2020>, last access: October 2021.
- Ajami, H, Sharma, A, Band, LE, Evans, JP, Tuteja, NK, Amirthanathan, GE, Bari, MA, 2017. On the non-stationarity of hydrological response in anthropogenically unaffected catchments: an Australian perspective. *Hydrology and Earth System Sciences*, 21(1): 281-294.
<http://doi.org/10.5194/hess-21-281-2017>
- Amirthanathan, GE, Bari, MA, Woldemeskel, FM, Tuteja, NK, Feikema, PM, 2023. Regional significance of historical trends and step changes in Australian streamflow. *Hydrology and Earth System Sciences*, 27(1): 229-254. <http://doi.org/10.5194/hess-27-229-2023>
- Beringer, J, McHugh, I, Hutley, LB, Isaac, P, Kljun, N, 2017. Technical note: Dynamic INtegrated Gap-filling and partitioning for OzFlux (DINGO). *Biogeosciences*, 14(6): 1457-1460.
<http://doi.org/10.5194/bg-14-1457-2017>
- Biancamaria, S, Lettenmaier, DP, Pavelsky, TM, 2016. The SWOT Mission and Its Capabilities for Land Hydrology. *Surveys in Geophysics*, 37(2): 307-337. <http://doi.org/10.1007/s10712-015-9346-y>
- BoM, 2020. Special Climate Statement 70—drought conditions in Australia and impact on water resources in the Murray–Darling Basin, Bureau of Meteorology, Australia, pp. 18.
<http://www.bom.gov.au/climate/current/statements/scs70.pdf>, last access: May 2023.
- BoM, 2021. National Groundwater Information System, Bureau of Meteorology.
<http://www.bom.gov.au/water/groundwater/ngis/>, last access: May 2023.
- Bretreger, D, Yeo, I, Hancock, G, Willgoose, G, 2020. Monitoring irrigation using Landsat observations and climate data over regional scales in the Murray-Darling Basin. *Journal of Hydrology*, 590. <http://doi.org/10.1016/j.jhydrol.2020.125356>
- Bretreger, D, Yeo, IY, Hancock, G, 2022. Corrigendum to: Monitoring irrigation using landsat observations and climate data over regional scales in the Murray-Darling Basin (vol 590, 125356, 2020). *Journal of Hydrology*, 608. <http://doi.org/10.1016/j.jhydrol.2022.127650>
- Budyko, MI, 1974. *Climate and Life*. Academic Press, New York, pp.,
- Chiew, FHS, 2006. Estimation of rainfall elasticity of streamflow in Australia. *Hydrological Sciences Journal*, 51(4): 613-625. <http://doi.org/10.1623/hysj.51.4.613>
- Chiew, FHS, Peel, MC, McMahan, TA, Siriwardena, LW (2006), Precipitation elasticity of streamflow in catchments across the world, Demuth, S., Gustard, A., Planos, E., Scatena, F., Servat, E. (Eds.), *Climate Variability and Change - Hydrological Impacts - 5th FRIEND World Conference*, Havana, Cuba, November 2006, 256-262,
<https://iahs.info/uploads/dms/13670.49-256-262-08-308-Chiew.pdf>
- Chiew, FHS, Potter, NJ, Vaze, J, Petheram, C, Zhang, L, Teng, J, Post, DA, 2014. Observed hydrologic non-stationarity in far south-eastern Australia: implications for modelling and prediction. *Stochastic Environmental Research and Risk Assessment*, 28(1): 3-15.
<http://doi.org/10.1007/s00477-013-0755-5>

- Chiew, FHS, Weber, TR, Aryal, SK, Post, DA, Vaze, J, Zheng, H, Peña Arancibia, JL, Robertson, DE, 2022. Evaluation of causes of reduced flow in the northern Murray–Darling Basin. CSIRO Technical report for the Murray–Darling Basin Authority., pp. 62.
<https://getinvolved.mdba.gov.au/56707/widgets/396639/documents/251893>, last access: May 2023.
- Crosbie, R, Wang, B, Kim, S, Mateo, C, Vaze, J, 2023. Changes in the surface water – Groundwater interactions of the Murray-Darling basin (Australia) over the past half a century. *Journal of Hydrology*, 622: 129683. <http://doi.org/https://doi.org/10.1016/j.jhydrol.2023.129683>
- CSIRO and BoM, 2022. State of the Climate 2022, Commonwealth Scientific and Industrial Research Organisation and Bureau of Meteorology, Australia, pp. 28.
<http://www.bom.gov.au/state-of-the-climate/2022/documents/2022-state-of-the-climate-web.pdf>, last access: May 2023.
- De Kauwe, MG, Medlyn, BE, Knauer, J, Williams, CA, 2017. Ideas and perspectives: how coupled is the vegetation to the boundary layer? *Biogeosciences*, 14(19): 4435-4453.
<http://doi.org/10.5194/bg-14-4435-2017>
- Deb, P, Kiem, AS, Willgoose, G, 2019. Mechanisms influencing non-stationarity in rainfall-runoff relationships in southeast Australia. *Journal of Hydrology*, 571: 749-764.
<http://doi.org/10.1016/j.jhydrol.2019.02.025>
- Denissen, JMC, Teuling, AJ, Pitman, AJ, Koirala, S, Migliavacca, M, Li, WT, Reichstein, M, Winkler, AJ, Zhan, CH, Orth, R, 2022. Widespread shift from ecosystem energy to water limitation with climate change. *Nature Climate Change*, 12(7): 677-+. <http://doi.org/10.1038/s41558-022-01403-8>
- Dey, R, Gallant, AJE, Lewis, SC, 2020. Evidence of a continent-wide shift of episodic rainfall in Australia. *Weather and Climate Extremes*, 29. <http://doi.org/10.1016/j.wace.2020.100274>
- Donohue, RJ, Roderick, ML, McVicar, TR, 2011. Assessing the differences in sensitivities of runoff to changes in climatic conditions across a large basin. *Journal of Hydrology*, 406(3-4): 234-244. <http://doi.org/10.1016/j.jhydrol.2011.07.003>
- Evans, A, Jones, D, Smalley, R, Lellyett, S, 2020. An enhanced gridded rainfall analysis scheme for Australia. Bureau Research Report No. 041, Bureau of Meteorology, pp. 45.
<http://www.bom.gov.au/research/publications/researchreports/BRR-041.pdf>, last access: May 2023.
- Fowler, K, Knoben, WJM, Peel, MC, Peterson, TJ, Ryu, D, Saft, M, Seo, KW, Western, A, 2020. Many Commonly Used Rainfall-Runoff Models Lack Long, Slow Dynamics: Implications for Runoff Projections. *Water Resources Research*, 56(5). <http://doi.org/10.1029/2019WR025286>
- Fowler, K et al., 2022. Explaining changes in rainfall–runoff relationships during and after Australia's Millennium Drought: a community perspective. *Hydrol. Earth Syst. Sci.*, 26(23): 6073-6120. <http://doi.org/10.5194/hess-26-6073-2022>
- Frost, AJ, Shokri, A, 2021. The Australian Landscape Water Balance model (AWRA-L v7). Technical Description of the Australian Water Resources Assessment Landscape model version 7. Bureau of Meteorology Technical Report, Bureau of Meteorology (BoM), Australia, pp. 66.
https://awo.bom.gov.au/assets/notes/publications/AWRA-Lv7_Model_Description_Report.pdf, last access: May 2023.
- Frost, AJ, Shokri, A, Keir, G, Bahramian, K, Azarnivand, A, 2021. Evaluation of the Australian Landscape Water Balance model: AWRA-L v7. Bureau of Meteorology Technical Report, Bureau of Meteorology (BoM), Australia, pp. 112.
https://awo.bom.gov.au/assets/notes/publications/AWRA-Lv7_Model_Evaluation_Report.pdf, last access: May 2023.

- Fu, GB, Chiew, FHS, Post, DA, 2023. Trends and variability of rainfall characteristics influencing annual streamflow: A case study of southeast Australia. *International Journal of Climatology*, 43(3): 1407-1430. <http://doi.org/10.1002/joc.7923>
- Fu, GB, Rojas, R, Gonzalez, D, 2022. Trends in Groundwater Levels in Alluvial Aquifers of the Murray-Darling Basin and Their Attributions. *Water*, 14(11). <http://doi.org/10.3390/w14111808>
- Fuentes, I, Scalzo, R, Vervoort, RW, 2021. Volume and uncertainty estimates of on-farm reservoirs using surface reflectance and LiDAR data. *Environmental Modelling & Software*, 143. <http://doi.org/10.1016/j.envsoft.2021.105095>
- GA, 2008. Mapping the growth, location, surface area and age of man made water bodies, including farm dams, in the Murray-Darling Basin, Geoscience Australia, Australia, pp. 83. https://www.mdba.gov.au/sites/default/files/archived/mdbc-RTSWR-reports/2136_Farm_Dams_in_the_MDB.pdf, last access: March 2022.
- Gallant, AJE, Kiem, AS, Verdon-Kidd, DC, Stone, RC, Karoly, DJ, 2012. Understanding hydroclimate processes in the Murray-Darling Basin for natural resources management. *Hydrology and Earth System Sciences*, 16(7): 2049-2068. <http://doi.org/10.5194/hess-16-2049-2012>
- Gardiya Weligamage, H, Fowler, K, Peterson, TJ, Saft, M, Peel, MC, Ryu, D, 2023. Partitioning of Precipitation Into Terrestrial Water Balance Components Under a Drying Climate. *Water Resources Research*, 59(5): e2022WR033538. <http://doi.org/https://doi.org/10.1029/2022WR033538>
- Goesch, T, Legg, P, Donoghoe, M, 2020. Murray–Darling Basin water markets: Trends and drivers 2002–03 to 2018–19, Australian Bureau of Agricultural and Resource Economics, Canberra, pp. 44. https://daff.ent.sirsidyntix.net.au/client/en_AU/search/asset/1029942/0, last access: June 2022.
- Grafton, RQ, Chu, L, Kingsford, RT, Bino, G, Williams, J, 2022. Resilience to hydrological droughts in the northern Murray-Darling Basin, Australia. *Philosophical Transactions of the Royal Society a-Mathematical Physical and Engineering Sciences*, 380(2238). <http://doi.org/10.1098/rsta.2021.0296>
- Guerschman, JP, McVicar, TR, Vleeshower, J, Van Niel, TG, Peña-Arancibia, JL, Chen, Y, 2022. Estimating actual evapotranspiration at field-to-continent scales by calibrating the CMRSET algorithm with MODIS, VIIRS, Landsat and Sentinel-2 data. *Journal of Hydrology*, 605. <http://doi.org/10.1016/j.jhydrol.2021.127318>
- Guo, D, Westra, S, Maier, HR, 2017. Sensitivity of potential evapotranspiration to changes in climate variables for different Australian climatic zones. *Hydrology and Earth System Sciences*, 21(4): 2107-2126. <http://doi.org/10.5194/hess-21-2107-2017>
- Habets, F, Molenat, J, Carluer, N, Douez, O, Leenhardt, D, 2018. The cumulative impacts of small reservoirs on hydrology: A review. *Science of the Total Environment*, 643: 850-867. <http://doi.org/10.1016/j.scitotenv.2018.06.188>
- Holgate, CM, van Dijk, AIJM, Evans, JP, Pitman, AJ, 2020. Local and Remote Drivers of Southeast Australian Drought. *Geophysical Research Letters*, 47(18). <http://doi.org/10.1029/2020GL090238>
- Kendall, MG, 1975. Rank Correlation Methods. Charles Griffin & Co. Ltd, London, pp. 202.
- King, AD, Klingaman, NP, Alexander, LV, Donat, MG, Jourdain, NC, Maher, P, 2014. Extreme Rainfall Variability in Australia: Patterns, Drivers, and Predictability. *Journal of Climate*, 27(15): 6035-6050. <http://doi.org/10.1175/Jcli-D-13-00715.1>
- Knyazikhin, Y, Martonchik, JV, Myneni, RB, Diner, DJ, Running, SW, 1998. Synergistic algorithm for estimating vegetation canopy leaf area index and fraction of absorbed photosynthetically active radiation from MODIS and MISR data. *Journal of Geophysical Research-Atmospheres*, 103(D24): 32257-32275. <http://doi.org/10.1029/98jd02462>

- Leblanc, MJ, Tregoning, P, Ramillien, G, Tweed, SO, Fakes, A, 2009. Basin-scale, integrated observations of the early 21st century multiyear drought in southeast Australia. *Water Resources Research*, 45. <http://doi.org/10.1029/2008wr007333>
- Li, BL, Rodell, M, Kumar, S, Beaudoin, HK, Getirana, A, Zaitchik, BF, de Goncalves, LG, Cossetin, C, Bhanja, S, Mukherjee, A, Tian, SY, Tangdamrongsub, N, Long, D, Nanteza, J, Lee, J, Policelli, F, Goni, IB, Daira, D, Bila, M, de Lannoy, G, Mocko, D, Steele-Dunne, SC, Save, H, Bettadpur, S, 2019. Global GRACE Data Assimilation for Groundwater and Drought Monitoring: Advances and Challenges. *Water Resources Research*, 55(9): 7564-7586. <http://doi.org/10.1029/2018wr024618>
- Lucas, R, Mueller, N, Siggins, A, Owers, C, Clewley, D, Bunting, P, Kooymans, C, Tissott, B, Lewis, B, Lymburner, L, Metternicht, G, 2019. Land Cover Mapping using Digital Earth Australia. *Data*, 4(4). <http://doi.org/10.3390/data4040143>
- Malerba, ME, Wright, N, Macreadie, PI, 2021. A Continental-Scale Assessment of Density, Size, Distribution and Historical Trends of Farm Dams Using Deep Learning Convolutional Neural Networks. *Remote Sensing*, 13(2). <http://doi.org/10.3390/rs13020319>
- McVicar, TR, Roderick, ML, Donohue, RJ, Van Niel, TG, 2012. Less bluster ahead? Ecohydrological implications of global trends of terrestrial near-surface wind speeds. *Ecohydrology*, 5(4): 381-388. <http://doi.org/10.1002/eco.1298>
- MDBA, 2018. Hydrologic assessment of flow changes in the northern Basin, Murray–Darling Basin Authority, Canberra, Australia, pp. 46. <https://www.mdba.gov.au/sites/default/files/pubs/1209-Hydrologic-assessment-of-flow-changes-in-the-northern-basin.pdf>, last access: May 2023.
- MDBA, 2022. Annual Water Take Report 2020–2021. Report on Basin wide water availability, use and Cap compliance, Murray–Darling Basin Authority, pp. 141. <https://www.mdba.gov.au/sites/default/files/pubs/annual-water-take-report-2020-21.pdf>, last access: May 2023.
- Morden, R, Horne, A, Bond, NR, Nathan, R, Olden, JD, 2022. Small artificial impoundments have big implications for hydrology and freshwater biodiversity. *Frontiers in Ecology and the Environment*. <http://doi.org/10.1002/fee.2454>
- Morton, FI, 1983. Operational estimates of areal evapotranspiration and their significance to the science and practice of hydrology. *Journal of Hydrology*, 66(1-4): 1-76. [http://doi.org/10.1016/0022-1694\(83\)90177-4](http://doi.org/10.1016/0022-1694(83)90177-4)
- Muñoz-Sabater, J, Dutra, E, Agustí-Panareda, A, Albergel, C, Arduini, G, Balsamo, G, Boussetta, S, Choulga, M, Harrigan, S, Hersbach, H, Martens, B, Miralles, DG, Piles, M, Rodriguez-Fernandez, NJ, Zsoter, E, Buontempo, C, Thepaut, JN, 2021. ERA5-Land: a state-of-the-art global reanalysis dataset for land applications. *Earth System Science Data*, 13(9): 4349-4383. <http://doi.org/10.5194/essd-13-4349-2021>
- Nguyen, H, Wheeler, MC, Hendon, HH, Lim, EP, Otkin, JA, 2021. The 2019 flash droughts in subtropical eastern Australia and their association with large-scale climate drivers. *Weather and Climate Extremes*, 32. <http://doi.org/10.1016/j.wace.2021.100321>
- Nicholls, N, Drosowsky, W, Lavery, B, 1997. Australian rainfall variability and change. *Weather*, 52: 66-71. <http://doi.org/10.1002/j.1477-8696.1997.tb06274.x>
- Parker, T, Gallant, A, Hobbins, M, Hoffmann, D, 2021. Flash drought in Australia and its relationship to evaporative demand. *Environmental Research Letters*, 16(6). <http://doi.org/10.1088/1748-9326/abfe2c>
- Peña-Arancibia, JL, Mainuddin, M, Kirby, JM, Chiew, FHS, McVicar, TR, Vaze, J, 2016. Assessing irrigated agriculture's surface water and groundwater consumption by combining satellite remote sensing and hydrologic modelling. *Science of the Total Environment*, 542: 372-382. <http://doi.org/10.1016/j.scitotenv.2015.10.086>

- Peña-Arancibia, JL, Malerba, ME, Wright, N, Robertson, DE, under review. Characterising the regional expansion of on-farm storages and their implications for water resources in the light of climate change *Journal of Hydrology*.
- Peña-Arancibia, JL, McVicar, TR, Paydar, Z, Li, LT, Guerschman, JP, Donohue, RJ, Dutta, D, Podger, GM, van Dijk, AIJM, Chiew, FHS, 2014. Dynamic identification of summer cropping irrigated areas in a large basin experiencing extreme climatic variability. *Remote Sensing of Environment*, 154: 139-152. <http://doi.org/10.1016/j.rse.2014.08.016>
- Peña Arancibia, JL, McVicar, TR, Kong, DD, Guerschman, JP, Van Niel, TG, Vleeshouwer, J, Li, LT, 2021. On the interchangeability of Landsat and MODIS data in the CMRSET actual evapotranspiration model – comment on “Monitoring Irrigation Using Landsat Observations and Climate Data over Regional Scales in the Murray-Darling Basin” by David Bretreger, In-Young Yeo, Greg Hancock and Garry Willgoose. *Journal of Hydrology*. <http://doi.org/10.1016/j.jhydrol.2021.127044>
- Peterson, TJ, Saft, M, Peel, MC, John, A, 2021. Watersheds may not recover from drought. *Science*, 372(6543): 745-749. <http://doi.org/doi:10.1126/science.abd5085>
- Pilgrim, DH, Chapman, TG, Doran, DG, 1988. Problems of Rainfall-Runoff Modeling in Arid and Semiarid Regions. *Hydrological Sciences Journal-Journal Des Sciences Hydrologiques*, 33(4): 379-400. <http://doi.org/10.1080/02626668809491261>
- Post, DA, Timbal, B, Chiew, FHS, Hendon, HH, Nguyen, H, Moran, R, 2014. Decrease in southeastern Australian water availability linked to ongoing Hadley cell expansion. *Earths Future*, 2(4): 231-238. <http://doi.org/10.1002/2013ef000194>
- Potter, NJ, Chiew, FHS, Frost, AJ, 2010. An assessment of the severity of recent reductions in rainfall and runoff in the Murray-Darling Basin. *Journal of Hydrology*, 381(1-2): 52-64. <http://doi.org/10.1016/j.jhydrol.2009.11.025>
- Rassam, DW, Pagendam, D, Gilfedder, M, Zhang, L, 2017. Non-stationarity of low flows and their relevance to river modelling during drought periods. *Marine and Freshwater Research*, 68(12): 2306-2314. <http://doi.org/10.1071/Mf16399>
- Rifai, SW, De Kauwe, MG, Ukkola, AM, Cernusak, LA, Meir, P, Medlyn, BE, Pitman, AJ, 2022. Thirty-eight years of CO2 fertilization has outpaced growing aridity to drive greening of Australian woody ecosystems. *Biogeosciences*, 19(2): 491-515. <http://doi.org/10.5194/bg-19-491-2022>
- Robertson, DE, Zheng, HX, Peña-Arancibia, JL, Chiew, FHS, Aryal, S, Malerba, ME, N., W, forthcoming. How sensitive are catchment runoff estimates to on-farm storages under current and future climates? *Journal of Hydrology*.
- Roderick, ML, Farquhar, GD, 2011. A simple framework for relating variations in runoff to variations in climatic conditions and catchment properties. *Water Resources Research*, 47. <http://doi.org/10.1029/2010wr009826>
- Rodriguez-Iturbe, I, D'Odorico, P, Porporato, A, Ridolfi, L, 1999. On the spatial and temporal links between vegetation, climate, and soil moisture. *Water Resources Research*, 35(12): 3709-3722. <http://doi.org/10.1029/1999wr900255>
- Saft, M, Peel, MC, Western, AW, Zhang, L, 2016. Predicting shifts in rainfall-runoff partitioning during multiyear drought: Roles of dry period and catchment characteristics. *Water Resources Research*, 52(12): 9290-9305. <http://doi.org/10.1002/2016wr019525>
- Schumacher, M, Forootan, E, van Dijk, AIJM, Mueller Schmied, H, Crosbie, RS, Kusche, J, Doll, P, 2018. Improving drought simulations within the Murray-Darling Basin by combined calibration/assimilation of GRACE data into the WaterGAP Global Hydrology Model. *Remote Sensing of Environment*, 204: 212-228. <http://doi.org/10.1016/j.rse.2017.10.029>
- Sen, PK, 1968. Estimates of Regression Coefficient Based on Kendall's Tau. *Journal of the American Statistical Association*, 63(324): 1379-&. <http://doi.org/10.2307/2285891>

- Tang, QH, Lettenmaier, DP, 2012. 21st century runoff sensitivities of major global river basins. *Geophysical Research Letters*, 39. <http://doi.org/10.1029/2011gl050834>
- Taschetto, AS, Stojanovic, M, Holgate, C, Drumond, A, Evans, J, Gimeno, L, Nieto, R, 2023. Reduced moisture sources contributed to the 2017-2019 southeast Australian drought. EGU General Assembly 2023. <http://doi.org/10.5194/egusphere-egu23-4681>
- Trancoso, R, Larsen, JR, McAlpine, C, McVicar, TR, Phinn, S, 2016. Linking the Budyko framework and the Dunne diagram. *Journal of Hydrology*, 535: 581-597. <http://doi.org/10.1016/j.jhydrol.2016.02.017>
- Ukkola, AM, Prentice, IC, Keenan, TF, van Dijk, AIJM, Viney, NR, Myneni, RB, Bi, J, 2016. Reduced streamflow in water-stressed climates consistent with CO2 effects on vegetation. *Nature Climate Change*, 6(1): 75-+. <http://doi.org/10.1038/Nclimate2831>
- van Dijk, AIJM, Beck, HE, Crosbie, RS, de Jeu, RAM, Liu, YY, Podger, GM, Timbal, B, Viney, NR, 2013. The Millennium Drought in southeast Australia (2001-2009): Natural and human causes and implications for water resources, ecosystems, economy, and society. *Water Resources Research*, 49(2): 1040-1057. <http://doi.org/10.1002/wrcr.20123>
- van Dijk, AIJM, Renzullo, LJ, Rodell, M, 2011. Use of Gravity Recovery and Climate Experiment terrestrial water storage retrievals to evaluate model estimates by the Australian water resources assessment system. *Water Resources Research*, 47. <http://doi.org/10.1029/2011wr010714>
- Verdon-Kidd, DC, Kiem, AS, 2009. Nature and causes of protracted droughts in southeast Australia: Comparison between the Federation, WWII, and Big Dry droughts. *Geophysical Research Letters*, 36. <http://doi.org/10.1029/2009gl041067>
- Verhoeven, E, Wardle, GM, Roth, GW, Greenville, AC, 2022. Characterising the spatiotemporal dynamics of drought and wet events in Australia. *Science of the Total Environment*, 846. <http://doi.org/10.1016/j.scitotenv.2022.157480>
- Wentworth Group of Concerned Scientists, 2020. Assessment of river flows in the Murray-Darling Basin: Observed versus expected flows under the Basin Plan 2012-2019., Wentworth Group of Concerned Scientists, Sydney, Australia, pp. 37. <https://wentworthgroup.org/wp-content/uploads/2020/08/MDB-flows.pdf>, last access: May 2023.
- Whetton, P, Chiew, F, 2021. Chapter 12 - Climate change in the Murray–Darling Basin. In: *Murray-Darling Basin, Australia*, Hart, B.T., Bond, N.R., Byron, N., Pollino, C.A., Stewardson, M.J. (Eds.). Elsevier, pp. 253-274. <http://doi.org/https://doi.org/10.1016/B978-0-12-818152-2.00012-7>
- Wiese, DN, Landerer, FW, Watkins, MM, 2016. Quantifying and reducing leakage errors in the JPL RL05M GRACE mascon solution. *Water Resources Research*, 52(9): 7490-7502. <http://doi.org/10.1002/2016wr019344>
- Winkler, AJ, Myneni, RB, Hannart, A, Sitch, S, Haverd, V, Lombardozzi, D, Arora, VK, Pongratz, J, Nabel, JEMS, Goll, DS, Kato, E, Tian, HQ, Arneth, A, Friedlingstein, P, Jain, AK, Zaehle, S, Brovkin, V, 2021. Slowdown of the greening trend in natural vegetation with further rise in atmospheric CO2. *Biogeosciences*, 18(17): 4985-5010. <http://doi.org/10.5194/bg-18-4985-2021>
- WMO, 2017. WMO Guidelines on the Calculation of Climate Normals, World Meteorological Organization (WMO), Switzerland, pp. 29. https://library.wmo.int/doc_num.php?explnum_id=4166, last access: May 2023.
- Zhang, YQ, Kong, DD, Gan, R, Chiew, FHS, McVicar, TR, Zhang, Q, Yang, YT, 2019. Coupled estimation of 500 m and 8-day resolution global evapotranspiration and gross primary production in 2002-2017. *Remote Sensing of Environment*, 222: 165-182. <http://doi.org/10.1016/j.rse.2018.12.031>

Zhao, M, Geruo, A, Liu, YL, Konings, AG, 2022. Evapotranspiration frequently increases during droughts. *Nature Climate Change*, 12(11): 1024-1030. <http://doi.org/10.1038/s41558-022-01505-3>

